260
3-8-77

Pr 770

DISTRIBUTION CATEGORY: UC64

APL/JHU/
AEO-76-066
NOVEMBER 1976

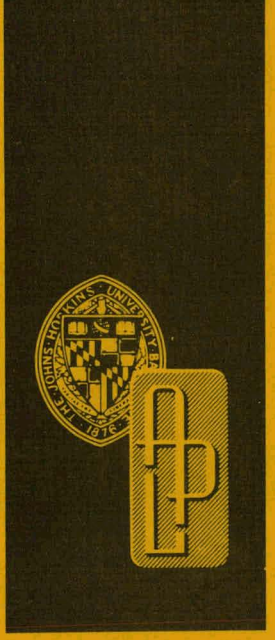

MASTER

INTERNAL HEAT TRANSFER EXPERIMENTS IN A SIMULATED OTEC EVAPORATOR TUBE

H. L. OLSEN, P. P. PANDOLFINI and J. L. RICE

Prepared by
THE JOHNS HOPKINS UNIVERSITY APPLIED PHYSICS LABORATORY
for the
DIVISION OF SOLAR ENERGY
U.S. ENERGY RESEARCH AND DEVELOPMENT ADMINISTRATION

REPORT PREPARED FOR TASK ZH9 UNDER
NAVY CONTRACT N00017-72-C-4401
WORK INITIATED APRIL 1976

THE JOHNS HOPKINS UNIVERSITY ■ APPLIED PHYSICS LABORATORY

DISTRIBUTION OF THIS DOCUMENT IS UNLIMITED

DISCLAIMER

This report was prepared as an account of work sponsored by an agency of the United States Government. Neither the United States Government nor any agency Thereof, nor any of their employees, makes any warranty, express or implied, or assumes any legal liability or responsibility for the accuracy, completeness, or usefulness of any information, apparatus, product, or process disclosed, or represents that its use would not infringe privately owned rights. Reference herein to any specific commercial product, process, or service by trade name, trademark, manufacturer, or otherwise does not necessarily constitute or imply its endorsement, recommendation, or favoring by the United States Government or any agency thereof. The views and opinions of authors expressed herein do not necessarily state or reflect those of the United States Government or any agency thereof.

DISCLAIMER

Portions of this document may be illegible in electronic image products. Images are produced from the best available original document.

This report was prepared as an account of work sponsored by the United States Government. Neither the United States nor the United States Energy Research and Development Administration, nor any of their employees, nor any of their contractors, subcontractors, or their employees, makes any warranty, express or implied, or assumes any legal liability or responsibility for the accuracy, completeness or usefulness of any information, apparatus, product or process disclosed, or represents that its use would not infringe privately owned rights.

Printed in the United States of America
Available from
National Technical Information Service
U.S. Department of Commerce
5285 Port Royal Road
Springfield, VA 22161
Price: Printed Copy $4.50; Microfiche $3.00

DISTRIBUTION CATEGORY: UC64

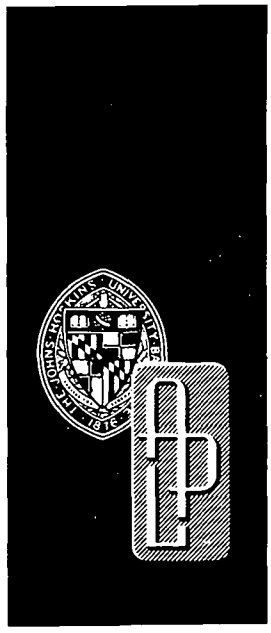

APL/JHU
AEO-76-066
NOVEMBER 1976

INTERNAL HEAT TRANSFER EXPERIMENTS IN A SIMULATED OTEC EVAPORATOR TUBE

H. L. OLSEN, P. P. PANDOLFINI and J. L. RICE

Prepared by
THE JOHNS HOPKINS UNIVERSITY APPLIED PHYSICS LABORATORY
for the
DIVISION OF SOLAR ENERGY
U.S. ENERGY RESEARCH AND DEVELOPMENT ADMINISTRATION

REPORT PREPARED FOR TASK ZH9 UNDER
NAVY CONTRACT N00017-72-C-4401
WORK INITIATED APRIL 1976

NOTICE
This report was prepared as an account of work sponsored by the United States Government. Neither the United States nor the United States Energy Research and Development Administration, nor any of their employees, nor any of their contractors, subcontractors, or their employees, makes any warranty, express or implied, or assumes any legal liability or responsibility for the accuracy, completeness or usefulness of any information, apparatus, product or process disclosed, or represents that its use would not infringe privately owned rights.

THE JOHNS HOPKINS UNIVERSITY ■ APPLIED PHYSICS LABORATORY

DISTRIBUTION OF THIS DOCUMENT IS UNLIMITED

THE JOHNS HOPKINS UNIVERSITY
APPLIED PHYSICS LABORATORY
LAUREL, MARYLAND

ABSTRACT

Internal heat transfer tests have been conducted by the Applied Physics Laboratory of The Johns Hopkins University (APL/JHU) for ammonia in two-phase flow inside a nearly horizontal 3-in.-diameter, 20-ft-long aluminum tube. This tube simulates one pass of a multipass evaporator tube for use in a low-cost ocean thermal energy conversion (OTEC) plant-ship concept developed by APL/JHU. The 29 tests covered mass flows of 1.0 to 2.8 lbm/sec, heat fluxes of 1100 to 2300 Btu/hr-ft^2 (provided by an external electric tape winding), qualities up to 20% vapor by mass (controlled by a steam-jacketed preheater), and tube angles varying from a 0.26° downward tilt to a 2.0° upward tilt in the flow direction. Results from the 16 tests in the final run at 2.0° upward tilt, for which accuracy is best because of added instrumentation, are in agreement with the Chaddock-Brunemann correlation for two-phase-flow heat transfer. This correlation relates the two-phase coefficients (h_1's) to the all-liquid convective coefficients (h_L's) (the Dittus-Boelter equation) through a function of the boiling number and the Martinelli parameter. Stratified wavy or intermittent flow occurred to some degree in all tests, and it is clear that a downward tilt, which could trap vapor bubbles, should be avoided. The results as a whole are judged to indicate that overall internal heat transfer coefficients essentially equivalent to the prior predictions for this heat exchanger concept will be obtained in evaporators using horizontal tubes. Additional tests, including tests at 0° tilt and at higher qualities, are desirable to substantiate this conclusion. Recommendations for further work are included.

TABLE OF CONTENTS

LIST OF ILLUSTRATIONS

List of Illustrations (Cont'd.) Page

LIST OF TABLES

1. INTRODUCTION

A critical element in the development of Ocean Thermal Energy Conversion (OTEC) plants is the design of heat exchangers capable of providing adequate heat transfer at minimal overall system cost. These OTEC heat exchangers must operate at low temperature differences (5 to 12°F) between the working fluid and seawater and must be designed to permit the periodic removal of biofouling which can degrade the heat exchanger performance. A promising low-cost heat exchanger concept is described in References 1-3, and additional background material is given in References 4-6. For both the evaporators and the condensers this concept employs large-diameter (3 to 4 in.) multipass aluminum tubes which contain ammonia as the working fluid. As shown in Fig. 1, the seawater is pumped to head ponds above these tube banks and flows through them by gravity. No heat exchanger shells are required; compartments in the concrete ship structure channel the water flow. In an evaporator, the ammonia is evaporated to approximately 60% mass quality as it rises through horizontal passes connected by return bends*. The vapor, separated from the liquid by a demister, drives the OTEC power turbine and is then condensed in downward flow through multiple horizontal passes. The liquid from the demister, together with the liquid from the bottom of the condenser, is pumped back into the evaporator.

Use of large tube diameters and nesting of several multipass tubes in one vertical plane to form an "element" results in a configuration which allows sufficient room between the vertical rows of the tube arrays to employ a low-cost system of water-jet cleaning heads to remove the biofouling from the outsides of the tubes. In addition, larger diameters permit a reduction in the number of joints needed to fabricate the heat exchangers, thus reducing fabrication costs.

Analyses of this configuration based upon available two-phase-flow heat transfer and pressure loss correlations indicated that the required heat exchange could be accomplished with low heat exchanger cost (References 2 and 3). This result, however, depends upon the validity of the correlations that have been employed--correlations which were obtained from experiments on smaller diameter tubes and at relatively high temperature differences. Therefore, experiments with larger diameter tubes and at heat inputs characteristic of OTEC operation were needed to validate the analyses and provide a firmer basis for the design of such heat exchangers. This report covers the initial experimental program, in which the ammonia-side heat transfer coefficients have been determined using an electrically heated tube, to simulate a single pass of evaporator tubing (20 ft long, horizontal, 3-in.-O.D. aluminum). Effects of flow rate, heat flux, and inlet quality (up to 20 mass percent vapor) have been evaluated, as well as effects of small changes in tube inclination on the degree of dryout at the top of the tube. The test equipment and operating procedures are described in Section 3. The results are presented and discussed in

*Figure 1 shows mitred bends for simplicity, but short-radius elbows are expected to be used in fabrication (Ref. 2).

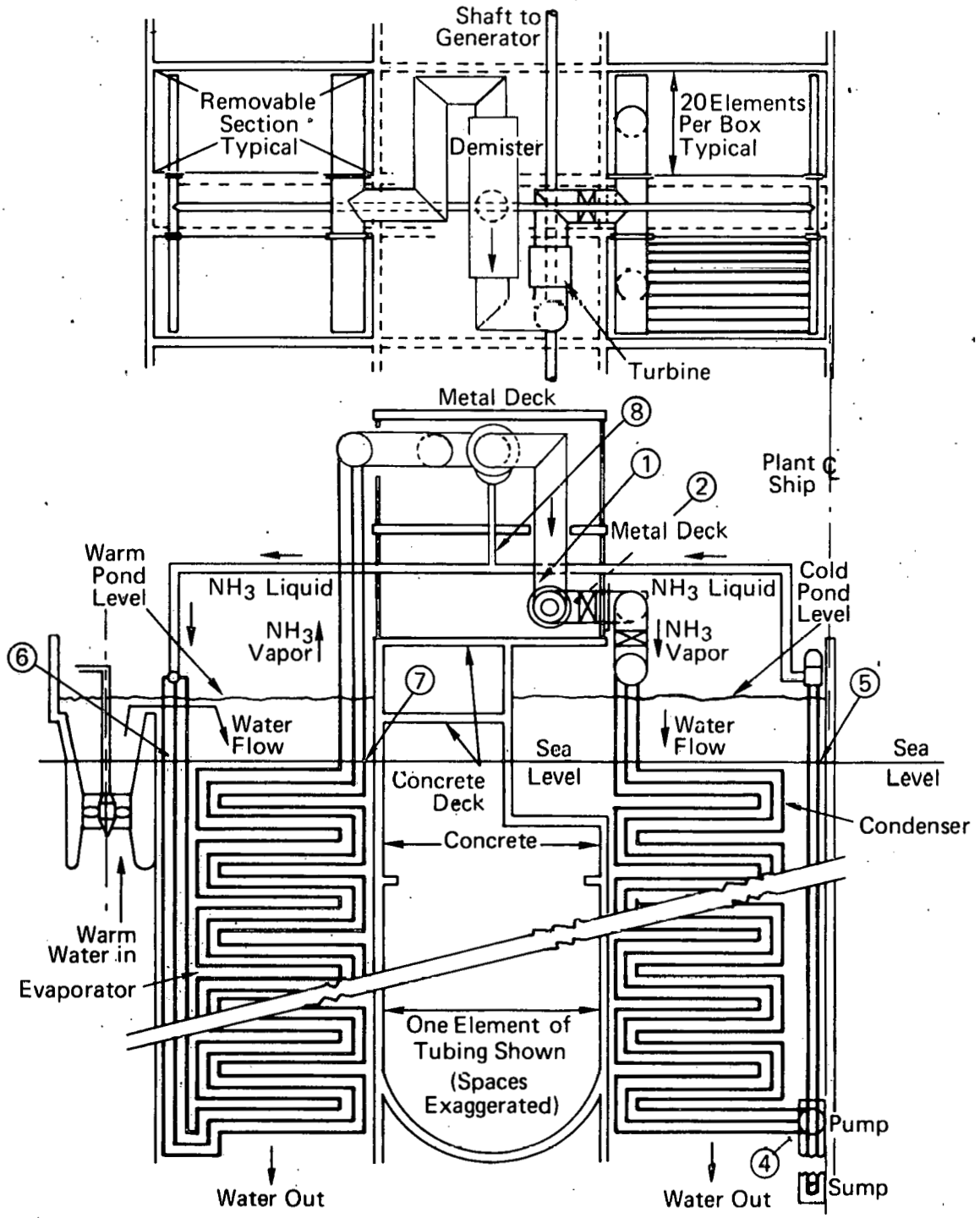

Fig. 1 Concept for Integrating a 5-MW_e (Net) Power Module with Heat Exchangers Made of Nested, Large-Diameter, Multipass Aluminum Tubes with a Modular, Barge-Type Platform for OTEC Plant-Ships.

Section 4. Conclusions and recommendations to proceed with tests of multi-pass tube models of both the evaporator and the condenser in a closed loop, and to conduct further tests with the present test loop, are presented in Section 5. Details of the preheater, demister and sump designs, the data reduction processes, and solution of the steady-state heat conduction equation are given in Appendices.

2. NOMENCLATURE

Upper Case

A_1, A_2	inside and outside surface areas, respectively (ft^2)
Bo	Boiling number, $\phi_1/i_g \rho_L V_L$
D_1, D_2	inside and outside diameters, respectively (ft)
P	measured static pressure (psia)
Pr	Prandtl number, $c_p \mu_L/k_L$
Re	Reynolds number, $D_1 V_L \rho_L/\mu_L$
T_{SAT}	saturation temperature (°F)
V_L	all-liquid velocity (ft/hr)
X_{tt}	Martinelli parameter (Eq. A-8, App. A)

Lower Case

c_p	specific heat of liquid (Btu/lbm-°F)
h_1	ammonia film heat transfer coefficient at inside wall (Btu/hr-ft^2-°F)
$h_{1(4)}$, $h_{1(3)}$	overall-tube-average h_1 (from all 3, 6, 9, and 12 o'clock values), and 3/4-tube-average (all 3, 6, and 9 o'clock values), respectively (Btu/hr-ft^2-°F)
h_{att}	heat transfer coefficient for attachment to outside wall (due to thermal contact resistance as a result of installation) for thermocouple or thermopile (Btu/hr-ft^2-°F)
h_L	all-liquid heat transfer coefficient per Dittus-Boelter equation (Btu/hr-ft^2-°F)

Nomenclature (cont'd.)

i_g	latent heat of vaporization (Btu/lbm)
k	thermal conductivity (Btu/hr-ft-°F)
r_1, r_2	inside and outside radii, respectively (ft)
t_2	outer wall temperature (°F)
t_{NH_3}	ammonia bulk temperature
$\dot{w}$	mass flow (lbm/sec)
x	quality, mass percent vapor (%)

Greek symbols

α	tube inclination angle (positive downward) (deg.)
ϕ_1, ϕ_2	heat fluxes at inner and outer walls, respectively (Btu/hr-ft^2)
μ_L	liquid viscosity (lbm/hr-ft)
ρ_L	liquid density (lbm/ft^3)
ΔT_{bulk}	temperature rise of ammonia from inlet to outlet of test section (°F)

3. DESCRIPTION OF THE EQUIPMENT

3.1 Experimental Setup

3.1.1 Overall Setup and Ammonia Circuit

The test loop is shown schematically in Fig. 2 and photographically in Figs. 3-6. Ammonia from a temperature-controlled storage tank is transferred (by nitrogen pressure) to fill the ammonia sump to an automatically-controlled head of 4 ft to preclude cavitation in the ammonia pump, which provides a constant mass flow rate. The ammonia pump is a double-sealed, positive-displacement, gear pump with a rated capacity of 30 gpm.* The pump is driven by a 3/4 H.P. electric motor through a Graham variable speed drive, which is used to vary the flow rate. A rotating vane flowmeter downstream of the pump measures the flow rate. The quality of the ammonia (mass percent vapor) entering the test section is changed by varying the heat input from a horizontal, steam-jacketed preheater described in Section 3.1.2 and Appendix A.

*Viking Heavy-Duty Refrigeration Ammonia Pump, Model K924, Viking Pump Division, Houdaille Industries, Inc., Cedar Falls, Iowa 50613

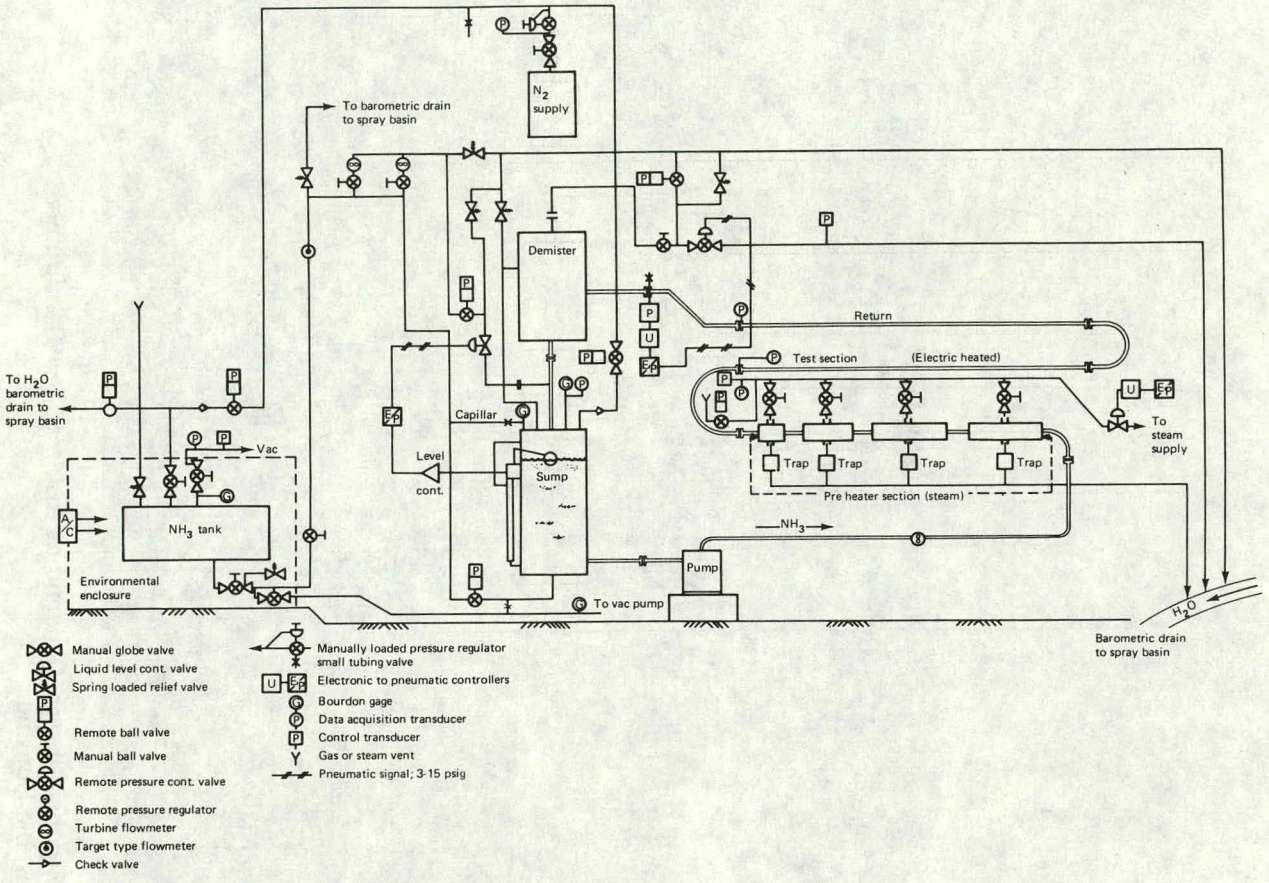

Fig. 2 Schematic Diagram of the Overall Setup for the OTEC Internal Flow Heat Transfer Experiment (IFHTE) Simulating a Single Evaporator Pass.

THE JOHNS HOPKINS UNIVERSITY
APPLIED PHYSICS LABORATORY
LAUREL, MARYLAND

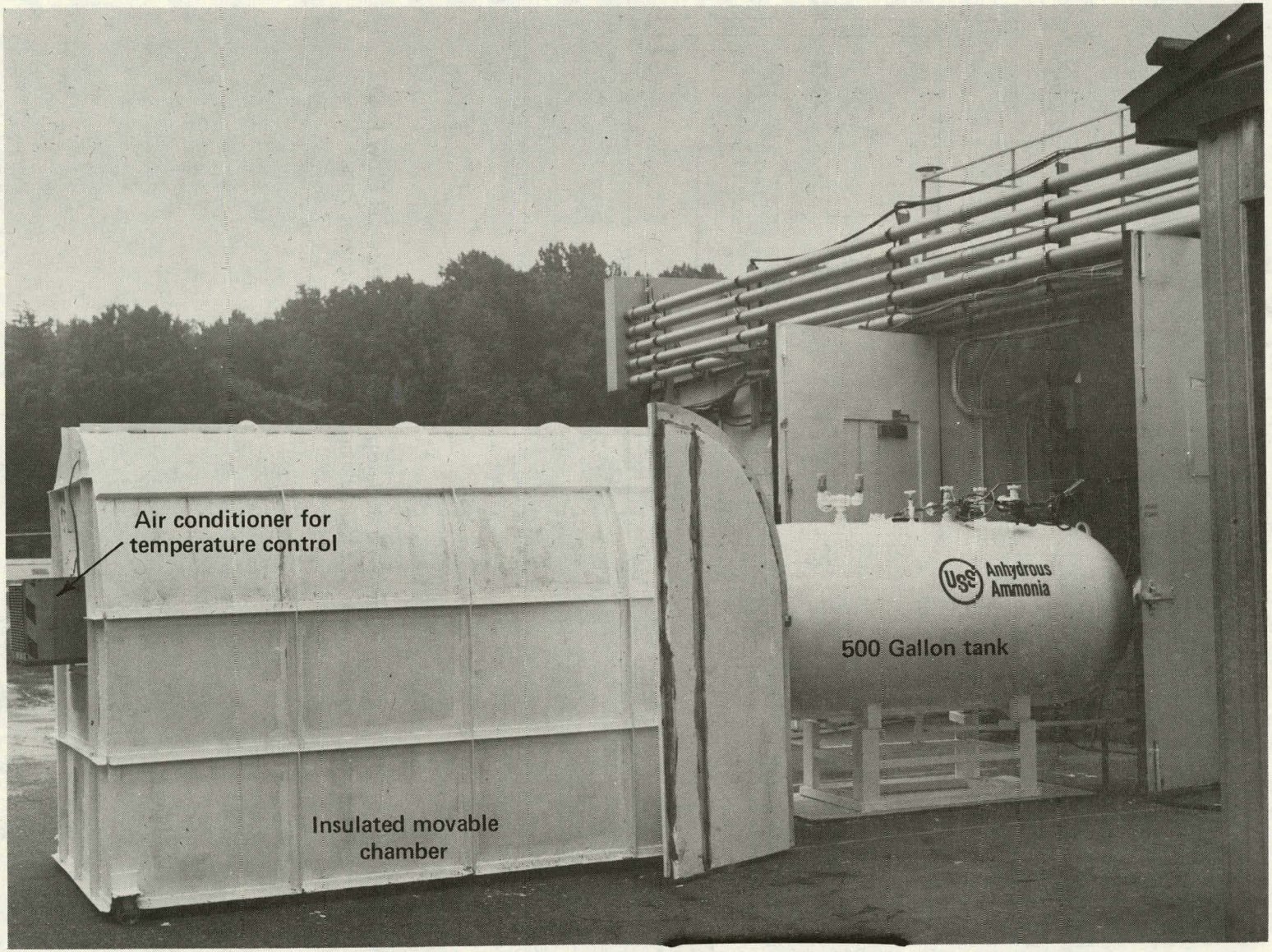

Fig. 3 Ammonia Storage Tank and its Insulated, Air-Conditioned, Movable Housing

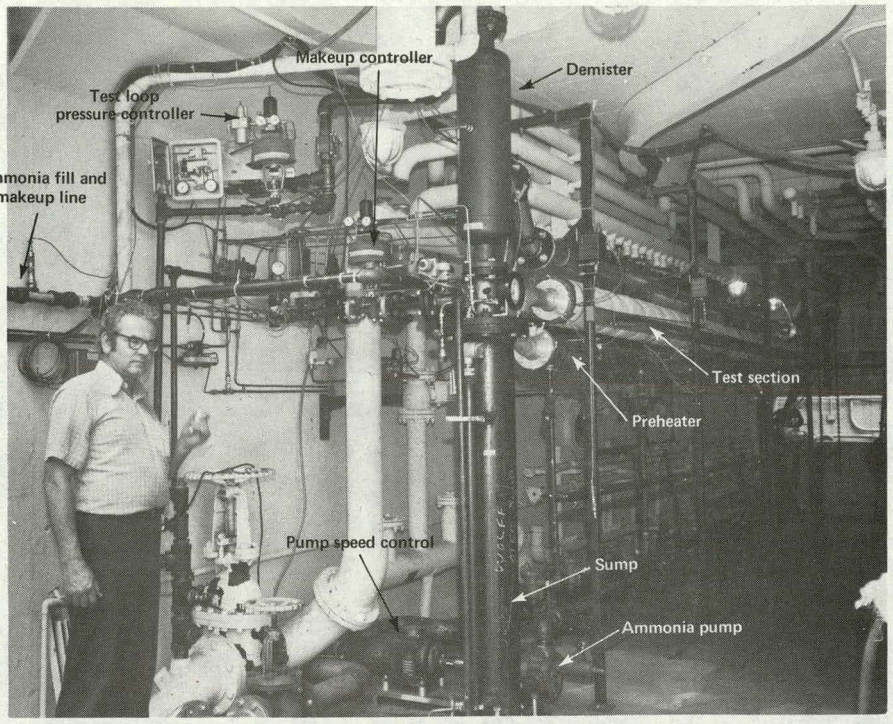

Fig. 4 OTEC/IFHTE Test Setup Viewed from Opened End of Test Cell

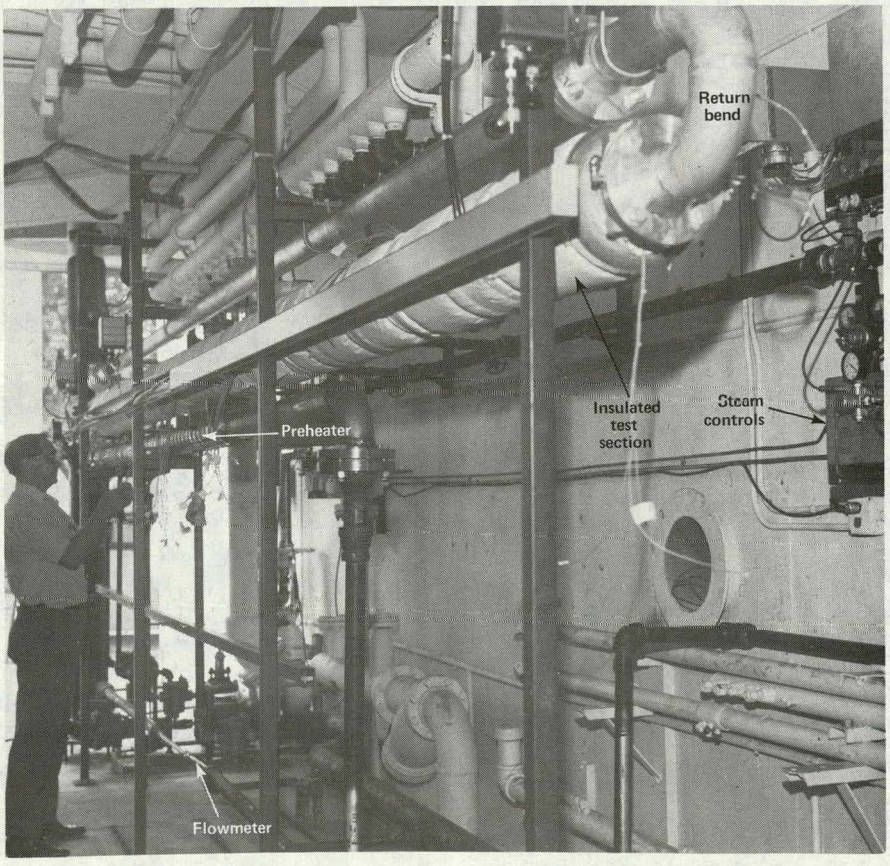

Fig. 5 OTEC/IFHTE Test Setup Viewed from Closed End of Test Cell

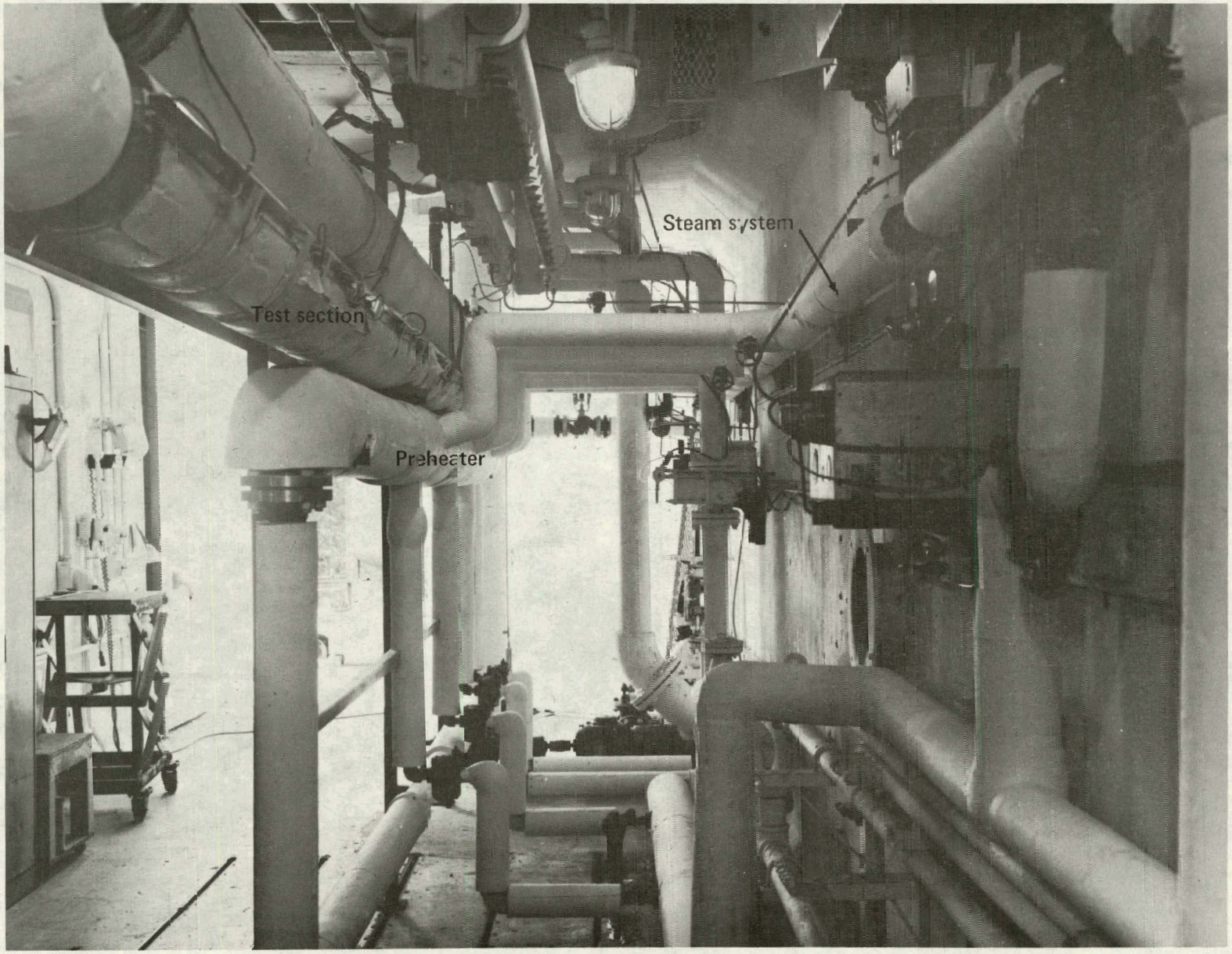

Fig. 6 OTEC/IFHTE Test Setup with Insulation on All Piping Surfaces Viewed from Closed End of Test Cell

The ammonia enters the horizontal (or slightly tilted) test section via a 180° return bend. The test section (described in Section 3.1.3) is wrapped with electric heating tape to provide a uniform external heat flux to the outside wall. The ammonia flows from the test section through a 180° bend and return line into a demister, which returns the liquid to the sump. The vapor is discarded via a pressure regulator into the facility water cooling system and escapes from a spray basin by gradual evaporation. This approach avoids the need for a large condenser in the loop. A pressure regulator controls the pressure at the demister inlet; its set point is remotely controlled. Liquid ammonia is added continuously to the sump to make up for the discarded vapor and maintain a constant sump level. For equilibrium conditions, the ratio of the measured ammonia makeup rate to the (constant) total pumping rate yields the ammonia quality x entering the demister, which is assumed to be equal to the quality leaving the test section.

The demister and sump are described in Appendix B. Further details on the preheater and test section follow.

3.1.2 Preheater Section

The 11-ft-long preheater is a 3-inch, schedule 80, stainless steel pipe equipped with end flanges and four steam jackets of lengths 1 ft, 2 ft, 4 ft, and 4 ft. Any desired combination of the steam jackets can be supplied with saturated steam at a controlled pressure ranging from 20 psia (T = 227°F) to 250 psia (T = 401°F). Thus, a wide range of heating rates up to 600,000 Btu/hr can be obtained, and ammonia quality can be controlled from a low level of 2% for an ammonia flow rate of 2500 lbm/hr to maxima ranging from 40% for 2500 lbm/hr to 10% for 10,000 lbm/hr. The preheater is connected to the test section inlet by a 9-inch center-to-center return bend. The heat transfer analysis used to size the preheater is presented in Appendix A.

3.1.3 Test Section

The test section is an aluminum T-6061 alloy tube of 3.021-inch outer diameter, 0.131-inch wall thickness and 20-ft length with a flange welded on each end. The inlet flange contains a static pressure tap at the 90° (3 o'clock, looking downstream) position, which is connected to a pressure transducer (PT2) at the same level as the tap, and a copper-constantan thermocouple at the 270° (9 o'clock) position. The thermocouple (TC2) is inserted* into the flow to measure the bulk temperature. Thermocouples and thermopiles are mounted on the outside wall of tube at measuring stations nominally 4 ft, 8 ft, 12 ft and 16 ft from the inlet flange as shown in Figs. 7-9. The tube is uniformly anodized in order to electrically isolate the thermopiles from the aluminum tube surface. After the instrumentation was installed, the tube is uniformly wrapped with 24

*Inserted to a depth to divide flow area into equal areas.

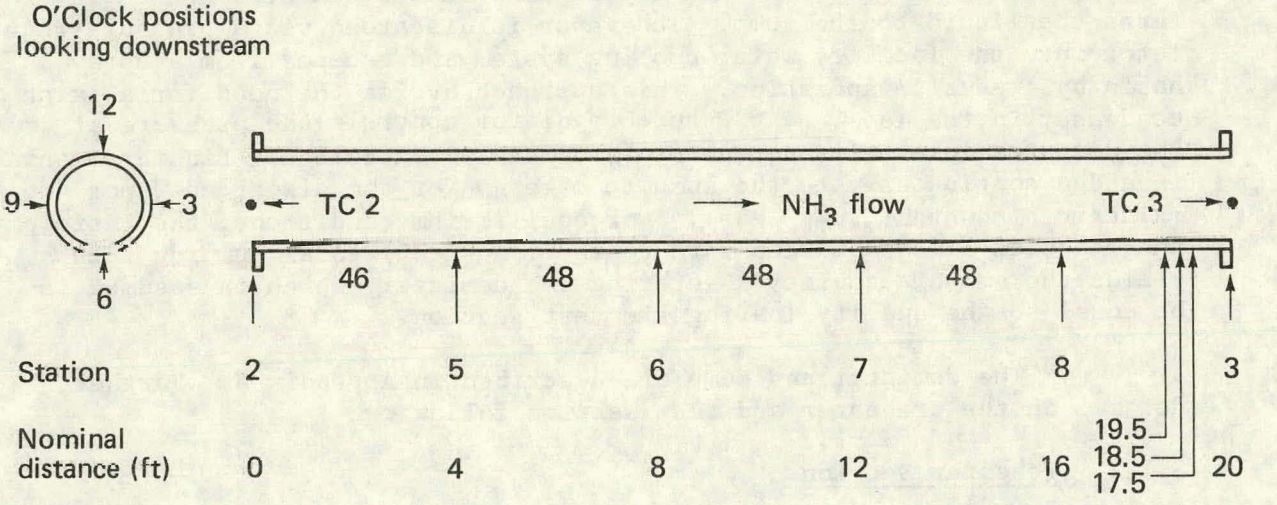

*Measured; + Interpolated

Test section tube characteristics

	Diameters	Heated surface area	Flow area
Outside	0.2518 ft.	$A_2 = 15.34\ ft^2$	–
Inside	0.23 ft	$A_1 = 14.01\ ft^2$	$A = 0.04155\ ft^2$

Heated length = 19.39 ft

Wall thickness = 0.131 ± 0.003 inch = 0.0109 ft (ave, 32 measurements)

Type material = T-6061 Aluminum alloy

Fig. 7 Simplified Schematic Diagram of OTEC/IFHTE Test Section Showing Instrumentation Stations and Positions, Geometric Data, and Interpolated Bulk Temperatures for Run 6, Test 2.

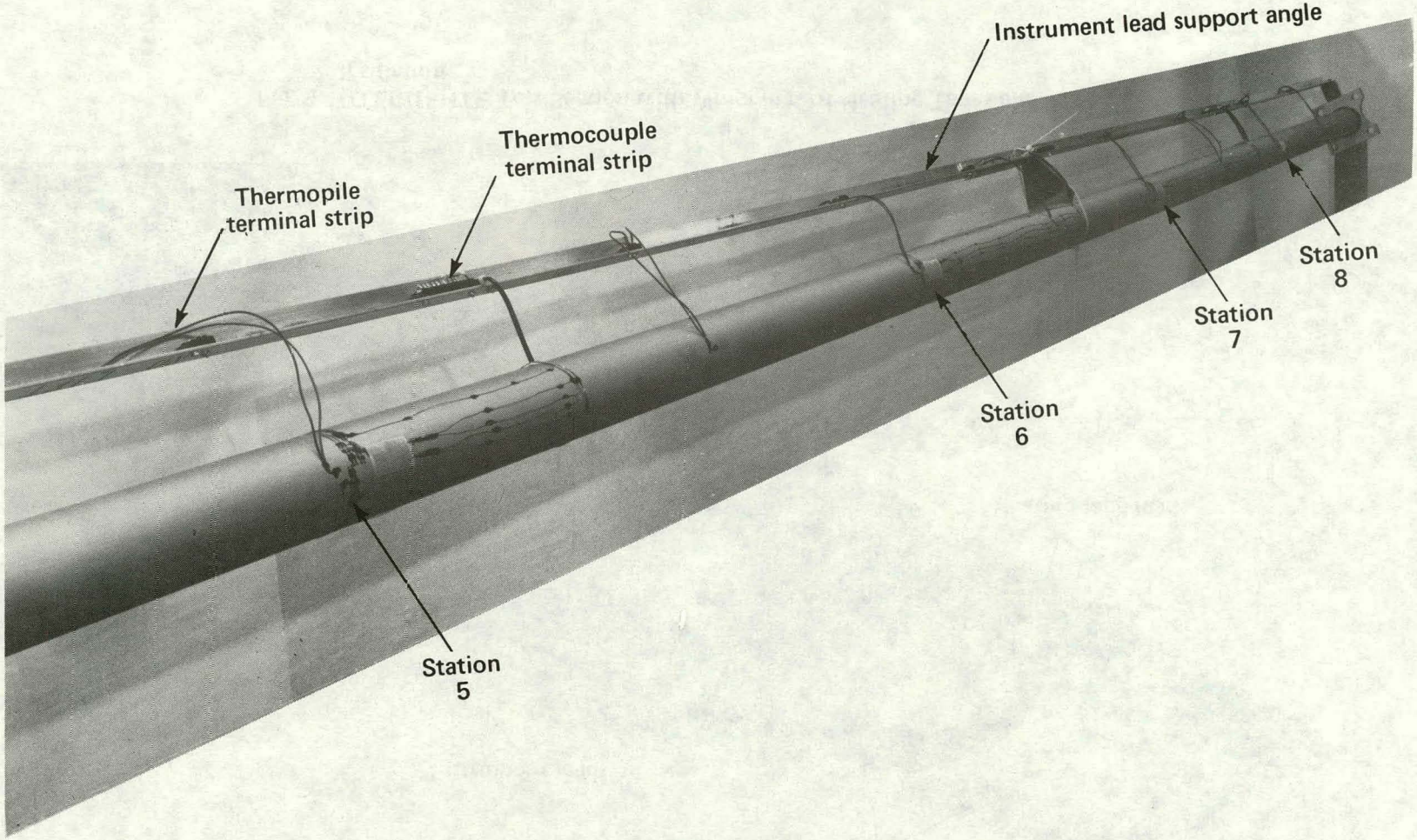

Fig. 8 OTEC/IFHTE Test Section with Thermocouples, Resistance Thermometers, and Thermopiles Mounted at Four Stations

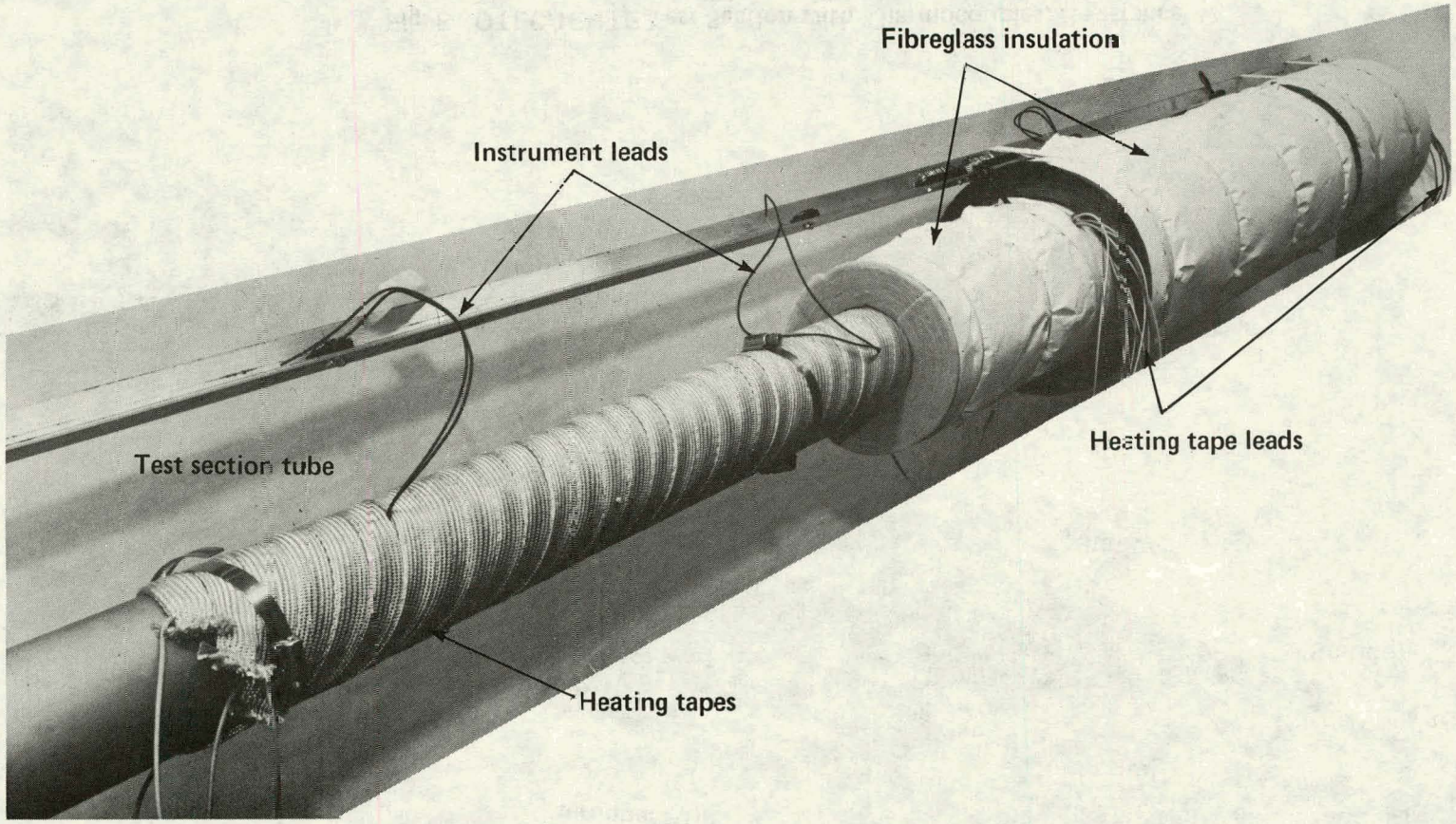

Fig. 9 OTEC/IFHTE Test Section with Wrappings of Heating Tapes and Insulation

heating tapes* as shown in Fig. 9, and finally covered with two layers of fiberglass insulation each 1.5 inch thick. An aluminum angle beam, bolted to the flanges and parallel to the tube as shown, was used to support the instrument leads and terminal strips.

A close, bottom view of one of the tube-wall instrumentation stations is shown in Fig. 10. A temperature reading at the bottom of the tube (6 o'clock position) is obtained from the copper-constantan thermocouple at A. This thermocouple has a round head of 0.030-in. diameter held into a slight depression (0.015 in.) in the anodized coating of the tube by a thin (1/2 mil) layer of Glyptal over the top of the bead. The leads near the bead are held in place by additional Glyptal and are insulated with teflon sleeves and connected to a terminal strip mounted on the aluminum angle. For the purpose of calibrating the thermocouples, each measuring station has a precision resistance thermometer attached at the 6 o'clock position adjacent to the thermocouples as shown at E of Fig. 10. Measurements from this station are obtained when the test section assembly is at thermal equilibrium and are used to calibrate the thermocouple output.

The tube wall temperatures at the 12-, 3-, and 9-o'clock positions are determined from differential temperatures referenced to the value measured at 6 o'clock. The differential temperatures are measured by four-junction thermopiles at B, C, and D of Fig. 10. The thermopile junctions are flat, butt-welded, 0.0002-in.-thick, copper-constantan elements that are pressed mechanically on the anodized surface and cemented in place by a thin (less than 1/2 mil) coat of Glyptal over the top of the junction. Each of these four-junction thermopiles has an output double that of a single junction thermocouple. The end leads are connected to the terminal strip.

The anodized surface was selected for electrically insulating the thermopile junctions from the aluminum tube surface because it is thin (approximately 0.0002-in. thick) and has both a high electrical resistance (approximately 10^6 ohms/cm^2) and a relatively high thermal conductivity (approximately 20 Btu/hr-ft-°F). However, as the testing progressed through the first five runs it was deduced from the data that significant thermal contact resistances existed for the majority of the thermocouples and thermopiles. Therefore, prior to run 6, three thermocouples were peened into the tube surface at the 6 o'clock position at stations 17.5, 18.5, and 19.5 inches upstream of the exit flanges as indicated in Fig. 7. The two leads for each couple were separately peened into holes drilled to 0.050-in. depth, 0.020-in. diameter, and 0.125-in. apart, so that the junction was made through the aluminum, and the teflon-sheathed leads could be brought out directly (perpendicularly) between turns of the heating tape. These three thermocouples provided very consistent readings, which were averaged to obtain a reference wall temperature in each test.

---

*Briskhead flexible heating tape, 1 in. x 8 ft, 1152 W, Cat. No. BWH-81-X, Briscoe Mfg. Co., Columbia, Ohio 43216

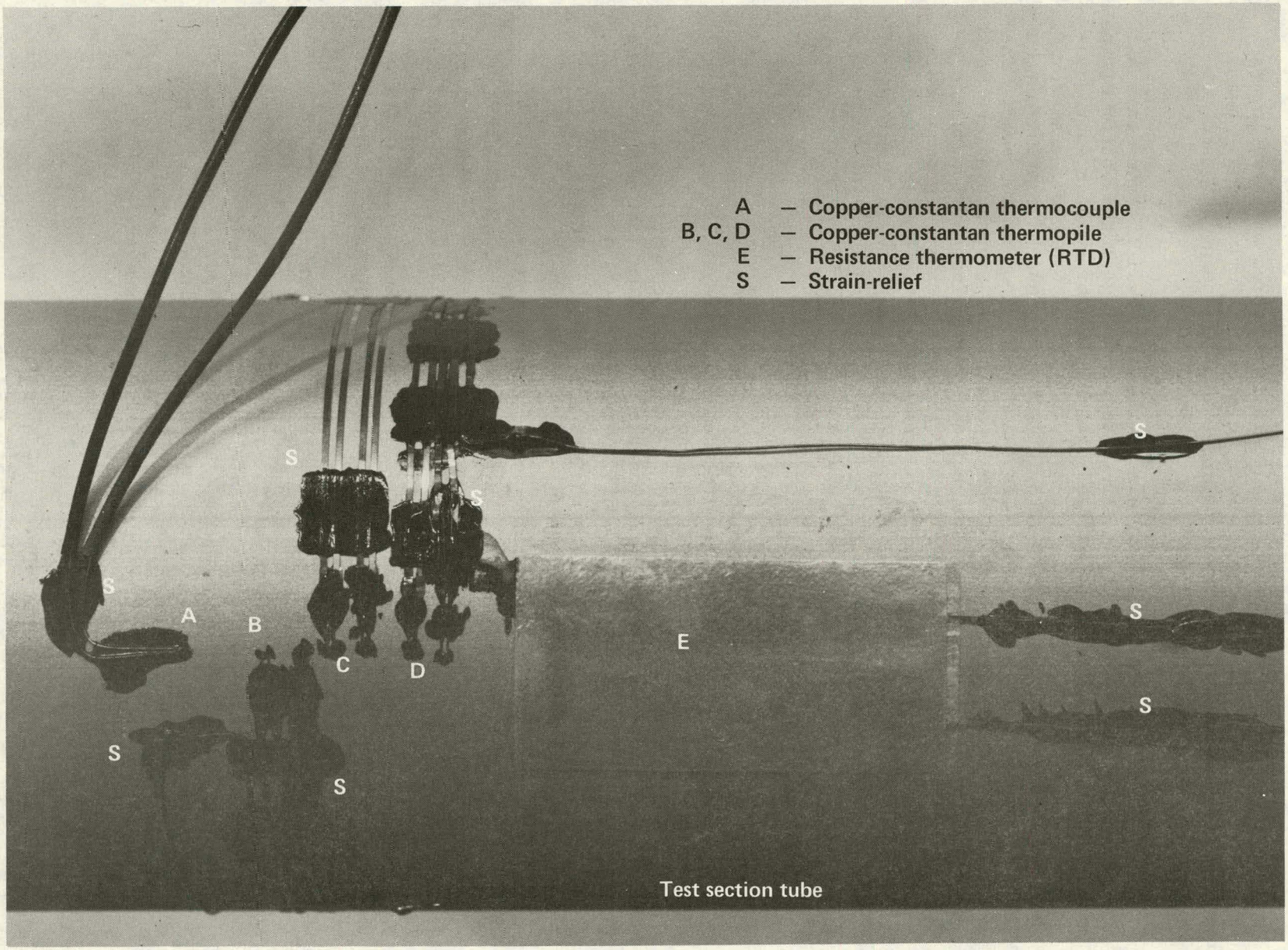

Fig. 10 Closeup of Instrumented OTEC/IFHTE Test Section Station at 6 o'clock Position

The latter temperature, in conjunction with the local ammonia bulk temperature, provided a basis for deducing the thermal contact resistances for the other wall temperature sensors as described in Section 4.2.

3.2 Test Procedures and Data Acquisition

The test loop is initially filled with ammonia by bypassing the ammonia supply line control valve until the correct liquid level is obtained in the sump. The ammonia pump is then started and the automatic level control system is allowed to draw additional liquid from storage to re-establish the required level in the sump. The flow in the ammonia supply line is measured by a rotating vane flowmeter whose output is integrated over a known period of time to provide the ammonia makeup flow rate. As previously noted, when an equilibrium condition is reached, the ratio of this ammonia supply rate (equal to the mass flow rate of the discarded ammonia vapor) to the flow rate through the pump gives the quality of the flow at the demister inlet.

In addition to the test section instruments and liquid level control already described, instrumentation was provided to measure storage tank pressure and temperature, sump pressure, demister inlet pressure, and heater tape voltage and current. The output signals of the various instruments are transmitted to the Digital Data Acquisition and Control System (DIDACS) for signal conditioning and for recording on magnetic tape during a test run. The test equipment is remotely controlled except for manual resetting of the valves of the steam jacket of the preheater and the setting of the ammonia pump speed. The system pressure at the demister inlet, the steam pressure, and the power to the test section heating tapes are controlled remotely. During the run, the system pressure, sump liquid level, main ammonia flow rate, makeup ammonia flow rate and steam pressure are monitored along with selected instrumentation readouts on temperature and pressure.

The sequential operations for a test are:

1. Fill the system with ammonia.
2. Open the manual steam valves for the desired combination of steam jackets.
3. Start the ammonia pump; adjust the Graham drive speed to yield the desired ammonia mass flow as indicated on the control panel flowmeter readout.
4. Adjust the demister inlet pressure to the desired saturation pressure for the run.

5. Adjust the storage tank pressure (by venting or adding nitrogen) from 1 to 2 psi above the saturation pressure.

6. Turn on the steam to the selected steam jacket(s) and adjust the steam pressure to the predetermined value.

7. Begin recording of data at predetermined intervals.

8. When the makeup ammonia flow rate becomes constant indicating that equilibrium conditions are achieved, turn on the power to the heating tapes and adjust the power supply voltage to the predetermined value.

9. When equilibrium has been attained again as evidenced by the readout becoming constant with passage of time and sufficient data recorded, turn off steam and heater tape power. When vapor is no longer vented, readjust the system for new run conditions or shut down operation.

The bulk of the data taken during the run is logged by DIDACS at one-minute intervals, sampling for a 5-sec period at a basic scan rate of 5 scans/sec. Logging sequences are continued until the makeup ammonia flow rate is constant, at which time equilibrium is deemed to have been reached. The heater tape power is then turned on and scan sequences are continued until a new equilibrium is achieved and for several intervals beyond equilibrium to provide statistically-useful data. The heater tape power is determined from strip-chart recordings of the power supply voltage and current, with allowance made for the measured lead resistance loss.

The magnetic tape from DIDACS is sent to the central computing center of APL for reduction of the data to printed format with measured quantities expressed in bits. For those logging sequences representing equilibrium flow conditions in the test loop, the bit readouts for each sequence are averaged (10 to 30 data scans). The average bit readout for each sensor is converted to engineering units by means of the calibration equation established for the sensor immediately prior to the run as described in Appendix C.

4. RESULTS

4.1 Run List

Table 1 summarizes the main conditions for each equilibrium test point in the runs conducted. Run 1 was a shakedown test. Runs 2 and 3 were conducted under nominal conditions and with the test section horizontal as measured with a spirit level. When the results indicated stratification, the test section inclination was measured with a transit,

Table 1. Run Summary

Run/ Test No.	Declination Angle (deg)[a]	NH_3 Flow Rate $\dot{w}$ (lbm/sec)	Inside Heat Flux ϕ_1 (Btu/hr-ft^2)	Quality (mass % vapor)	Pressures (psia) Test Section Inlet P_{TSIN}	Pressures (psia) Demister Inlet	Sat'n. Temp. Corresp. to P_{TSIN} T_{SAT} (°F)
1/ 1		(Shakedown Test)					
2/ 2	+0.26[a]	0.98	1193	2.7	132.9[c]	131.6[c]	71.8
3/ 1	+0.26	1.02	1139	0[b]	133.3	132.1	72.0
2		0.96	1125	4.7	132.5	131.7	71.6
3		0.97	1156	7.2	132.5	131.8	71.6
4		0.97	1154	19.9	132.8	131.7	71.7
5		1.55	1144	0	132.6	131.7	71.7
6		1.46	1152	14.8	132.5	131.7	71.6
4/ 1	-0.21	1.02	1209	0	132.6	131.8	71.7
2		1.95	1201	9.2	132.8	131.9	71.8
5/ 1	-0.21	2.59	1161	0	117.7	118.0	64.9
2		2.21	1188	7.7	117.4	117.6	64.8
3		2.20	2314	8.4	117.4	117.9	64.8
4		2.21	1192	8.9	127.4	128.3	69.4
6/ 1	-2.0	--	--	0[b]	--	--	
2		1.02	1112	0	113.8	113.3	63.1
3		1.01	2165	0	129.4	128.8	70.3
4		2.79	2165	0	129.4	129.0	70.3
5		2.80	1118	0	140.1	139.4	74.8
6		1.85	1118	0	153.8	152.5	80.3
7		1.84	2170	0	167.3	166.3	85.0
8		0.94	1169	5.5	126.7	126.4	69.1
9		0.94	1169	12.2	126.7	126.5	69.1
10		0.94	1169	18.1	126.7	126.4	69.1
11		2.77	1169	3.0	126.8	126.5	69.1
12		2.82	1169	6.2	126.9	126.4	69.2
13		2.81	1169	9.7	126.6	126.1	69.0
14		1.86	1169	11.2	126.6	126.0	69.0
15		1.86	1169	9.3	126.9	126.4	69.2
16		1.85	2170	8.1	126.7	126.4	69.1
17		1.84	2170	0	127.0	125.9	69.2

[a] A positive sign denotes a declining angle. This convention is used in some of the two-phase-flow literature (e.g., Ref. 7).

[b] A zero in the quality column indicates that no preheating was done and there was no ammonia makeup flow, i.e., an all-liquid-inlet test.

[c] Accuracy of pressure measurements is $\pm$ 0.5 to 1.0 psi. This means accuracy of T_{SAT} (from thermodynamic tables, Ref. 8) is $\pm$ 0.2-0.5°F.

and a declination, measured in the direction of flow, of +0.26° was found. The tube was therefore readjusted and runs 4 and 5 were carried out with a -0.21° test section declination angle α (+0.21° inclination; this convention for α follows Ref. 7) and with increased ammonia mass flow rates. Finally, run 6 was made, with the peened-in thermocouples mentioned in Section 3.1.3 installed, to determine the effects of mass flow, heat flux, and quality at a test section at α = -2.0°.

4.2 Deduced Outside Wall Temperature

The measured ammonia bulk temperatures, reference outside wall temperatures, and deduced outside wall temperatures are presented in Table 2. The second decimal places on the temperatures are not significant but are listed because they were used to compute the heat transfer coefficients. The headings in columns (4) through (23) indicate the test section positions as described in Fig. 7. The inlet and outlet stations where the ammonia bulk temperature was measured are designated as stations 2 and 3, respectively. Positions 5.6 and 5.3 are the 6 o'clock and 3 o'clock positions at station 5, respectively, and so on. The measurements from the three peened-in thermocouples at the 6 o'clock position at distances of 17.5, 18.5, and 19.5 inches from the exit are listed in columns (21) through (23). Their readings agree well, with an average deviation of 0.1°F.

The average of the temperatures indicated by these three peened-in thermocouples is taken to be the true surface temperature of the metal tube at the 6 o'clock position 18.5 in. from the exit, or 15 in. from the end of the heated section. With this datum, along with the bulk temperature of the liquid, which is assumed to vary linearly in temperature between the inlet and outlet, and the heat input from the tape wrapping the film coefficient of the liquid ammonia at this location can be calculated.

The values found from the all-liquid-inlet tests 2 through 6 and 17 of run 6 are listed in Table 3 in column 7 under the heading "Exp h_l." Since the flow is constant, and the heating rate is constant, the rate of heat transfer, and hence the temperature drop from the outside surface of the tube to the ammonia bulk flow, must also be constant along the tube. Thus, the outside wall temperature will rise linearly with distance along the tube as the liquid temperature rises due to heat absorbed from the heating tape. As mentioned in Section 3.1.3 the thermocouples and thermopiles which were cemented to the tube at stations 5, 6, 7 and 8 to provide data on longitudinal and circumferential variation in heat transfer yield temperature readings above the deduced outside wall temperature, which proves the existence of thermal resistances between the cemented junctions and the tube wall. Since the true wall temperature can be found by interpolation for these all-liquid tests, the thermal resistance associated with each thermocouple or thermopile junction can be estimated.

Table 2. Outside Wall Temperatures (^{o}F) Deduced from Primary Thermocouple (TC) and Thermopile (TP) Data[a]

(1)	(2)	(3)	(4)	(5)	(6)	(7)	(8)	(9)	(10)	(11)	(12)	(13)	(14)
			NH_3 Bulk TC										
Run	Test	Quality (%)	2	3	TC 5.6	TP 5.3	TP 5.9	TP 5.12	TC 6.6	TP 6.9	TP 6.12	TP 7.6	TP 7.3
2	1	2.7	72.66	73.66	73.51	73.55	73.60	89.79	74.39	76.83	92.96	74.97	77.72
3	1	0	73.15	74.90	74.47	75.44	75.84	91.68	75.61	75.79	87.59	76.82	76.48
	2	4.7	72.75	74.40	72.91	72.42	72.52	85.68	74.21	75.41	90.04	74.55	76.21
	3	7.2	72.59	74.14	72.97	71.96	72.66	84.94	73.85	74.36	89.38	74.37	76.08
	4	19.9	72.47	80.00	71.72	75.05	75.24	90.91	72.79	77.63	92.17	73.53	77.27
	5	0	73.27	75.13	73.17	74.67	75.30	91.39	74.37	77.31	94.90	75.96	76.28
	6	14.8	72.77	73.43	71.01	71.61	71.93	85.95	71.76	72.23	81.38	73.38	74.54
4	1	0	70.56	72.79	74.93	75.00	74.80	73.11	75.10	75.31	73.39	76.36	76.01
	2	9.2	70.60	70.98	71.05	71.39	70.49	81.16	71.66	70.49	77.66	71.88	70.98
5	1	0	64.73	66.12	63.92	64.13	63.91	64.98	65.40	65.68	64.32	66.78	66.74
	2	7.7	64.55	64.97	62.18	61.94	61.45	68.81	63.80	63.29	70.54	64.97	64.31
	3	8.4	64.39	64.69	62.31	62.92	61.01	83.76	64.09	62.61	80.71	66.13	64.71
	4	8.9	69.15	69.23	66.32	65.98	66.07	76.88	71.82	71.39	78.08	69.44	68.91
6	8	5.5	69.77	69.74	72.73	70.89	70.83	71.12	72.58	70.70	71.08	72.53	70.92
	9	12.2	69.66	69.53	72.80	71.20	71.16	71.59	72.79	71.40	71.20	72.37	70.80
	10	18.1	69.71	69.80	72.06	72.32	72.51	88.87	72.48	67.50	72.87	72.54	70.73
	11	3.0	69.74	69.71	71.61	71.31	71.21	71.92	71.72	71.06	71.49	71.70	71.32
	12	6.2	69.97	69.73	71.16	70.82	70.63	72.83	71.37	70.61	70.88	71.33	70.88
	13	9.7	70.05	69.87	71.10	71.10	70.79	76.11	71.50	71.11	71.59	71.36	70.81
	14	11.2	69.82	69.82	71.38	71.24	71.05	78.41	71.67	70.97	72.15	71.50	70.75
	15	9.3	69.91	70.08	71.61	71.01	71.02	76.38	71.84	71.11	71.14	71.89	70.93
	16	8.1	69.78	69.76	72.39	70.57	70.33	78.35	71.71	69.98	70.29	73.19	71.12

[a]Primary data are given in Table C-1, Appendix C. Data from the all-liquid-inlet tests 2-7 and 17 of run 6 are used for calibration; see text and Table 3.

THE JOHNS HOPKINS UNIVERSITY
APPLIED PHYSICS LABORATORY
LAUREL, MARYLAND

Table 2 (concluded)

(1)	(2)	(3)	(15)	(16)	(17)	(18)	(19)	(20)	(21)	(22)	(23)	(24)	(25)
									Peened-In Thermocouples				
Run	Test	Quality (%)	TP 7.9	TP 7.12	TC 8.6	TP 8.3	TP 8.9	TP 8.12	TC 17.5.6	TC 18.5.6	TC 19.5.6	Avg. (21) - (23)	V_L ft/hr
2	1	2.7	78.29	95.87	76.62	76.31	76.50	88.17	--	--	--	--	2230
3	1	0	76.64	84.11	78.18	78.05	77.90	74.18	--	--	--	--	2319
	2	4.7	77.76	93.25	75.34	71.82	79.29	95.13	--	--	--	--	2198
	3	7.2	76.35	92.28	75.04	69.47	81.11	95.50	--	--	--	--	2216
	4	19.9	79.24	93.83	74.42	68.84	80.48	94.87	--	--	--	--	2216
	5	0	76.09	83.93	77.29	76.42	77.75	82.15	--	--	--	--	3527
	6	14.8	72.95	87.31	73.85	72.62	75.46	89.34	--	--	--	--	3329
4	1	0	75.95	73.03	76.79	76.71	76.54	72.91	--	--	--	--	2319
	2	9.2	71.05	63.62	72.17	72.54	71.39	72.47	--	--	--	--	4437
5	1	0	66.86	66.34	67.39	67.07	67.71	67.10	--	--	--	--	5910
	2	7.7	64.28	65.89	65.64	65.97	65.06	66.00	--	--	--	--	5044
	3	8.4	64.19	67.84	66.79	67.34	65.16	67.90	--	--	--	--	5023
	4	8.9	68.50	75.27	70.13	70.39	69.33	70.74	--	--	--	--	5037
6	8	5.5	70.75	71.64	72.60	73.90	71.29	71.73	72.72	73.03	72.46	72.74	2146
	9	12.2	70.89	71.93	72.60	75.20	70.97	71.91	72.53	72.52	72.44	72.56	2136
	10	18.1	70.83	71.76	72.43	73.86	70.69	71.88	72.26	72.18	72.22	72.22	2134
	11	3.0	71.34	72.09	71.60	71.88	71.10	71.77	71.81	71.76	71.88	71.82	6316
	12	6.2	71.00	72.45	71.46	71.88	70.95	72.14	71.53	71.46	71.34	71.44	6418
	13	9.7	70.89	72.05	71.70	72.30	70.93	72.14	71.61	71.77	71.58	71.65	6402
	14	11.2	70.85	72.10	71.73	72.40	70.95	71.96	71.58	71.88	71.66	71.71	4248
	15	9.3	71.13	72.76	72.15	73.02	71.13	72.19	71.92	72.02	71.91	71.95	4239
	16	8.1	71.53	73.84	73.30	74.61	71.10	73.45	73.75	73.27	73.55	73.52	4225

THE JOHNS HOPKINS UNIVERSITY
APPLIED PHYSICS LABORATORY
LAUREL, MARYLAND

Table 3. Experimental Heat Transfer Coefficients for All-Liquid-Inlet Tests of Run 6 and Thermal Conductances Deduced for Thermocouple Junctions on Outside Wall at 6 O'Clock Positions.

Test	Outside Wall Heat Flux ϕ_2 Btu/hr-ft^2	V_L (ft/hr)	Ammonia Bulk Temp. TC 2(in) °F	Ammonia Bulk Temp. TC 3(out) °F	Outside Wall Temp. at Sta. 18.5.6[a] °F	Exp h_l Btu/hr-ft^2-°F	Deduced Thermal Conductance h_{att}, Btu/hr-ft^2-°F TC 5.6	TC 6.6	TC 7.6	TC 8.6
6/2	1016	2319	60.63	63.31	66.92	305	225	125	313	478
3	1977	2312	68.51	72.37	79.83	290	230	122	294	391
4	1977	6359	70.61	72.34	76.86	485	249	124	336	417
5	1021	6377	73.41	74.69	77.40	421	212	104	318	350
6	1021	4220	79.27	80.81	84.00	353	265	126	358	381
7	1982	4204	83.64	86.09	91.73	390	282	141	381	473
17	1982	4195	69.96	71.84	77.68	380	249	131	337	413
					Average h_{att}		244	125	334	415
					Standard Deviation		23	10	27	44
					For a heat flux ϕ_2 of 1015 Btu/hr-ft^2, Δt_{att} (°F) =		4.14	8.13	3.04	2.45
					And one standard deviation represents (°F):		+0.5 -0.4	+0.7 -0.6	+0.3 -0.2	+0.3 -0.2

[a] Average temperature from the three peened-in thermocouples taken to be true wall temperature at 6 o'clock position 18.5 in. upstream of exit plane. Individual readings are given in columns (21) - (23), Table C-1.

The thermal conductance coefficients (h_{att}'s) associated with the thermal resistances have been evaluated from the all-liquid-inlet tests of run 6, using the solution of the one-dimensional steady-state cylindrical conduction equation given in Appendix D. The results for the thermocouples at the 6 o'clock position are presented in Table 3. The derived values for a given thermocouple from successive tests are consistent, and do not show a trend with heat flux or flow velocity. The standard deviations are only 8% to 11%, representing small temperature differences. Thus, the mean values provide a suitable method for calibration of the instruments to use in determining the spatial variation of the two-phase-flow heat transfer coefficients. (The procedure for calculating the net value for the two attachments of a thermopile is more complex and is presented in Appendix C.)

In order to demonstrate this technique, consider the example of run 6, test 2 which is an all-liquid test (x = 0%) with the heating tapes putting 4563 watts (Q = 15574 Btu/hr) into the test section, so that ϕ_2, the heat flux at the outside tube surface is 1016 Btu/hr-ft^2, and ϕ_1 at the inside surface is 1112 Btu/hr-ft^2. The bulk temperature of the ammonia increases from 60.63°F at the test section inlet to 63.31°F at the outlet (Table 3). Because the heat flux is uniform, the bulk temperature can be assumed to increase uniformly along the tube; the interpolated bulk temperatures at the measuring stations are shown in Fig. 7. The average temperature of the peened-in thermocouples is 66.92°F; with the interpolated bulk temperature at that station (63.14°F), and the thermal conductivity (k) and geometric properties of the tube from Fig. 7, the following equation may be used to calculate the inside film heat transfer coefficient h_1:

$$\frac{1}{h_1} = \frac{t_2 - t_{NH_3}}{\phi_1} - \frac{r_1}{k} \ln \frac{r_2}{r_1} \qquad (1)$$

$$\frac{1}{h_1} = \frac{66.92-63.14}{1112} - \frac{0.115}{89.2} \ln \frac{0.1259}{0.115} = 0.00340-0.00012$$

$$h_1 = 305 \text{ Btu/hr-ft}^2\text{-°F}$$

Now consider the thermocouple at station 5.6. The local bulk temperature of the ammonia is 61.17°F; using h_1 = 305 Btu/hr-ft^2-°F and this t_{NH_3}, the outer tube surface temperature at this station is calculated from Eq. (1) solved for t_2:

$$t_2 = t_{NH_3} + \phi_1 \left(\frac{r_1}{k} \ln \frac{r_2}{r_1} + \frac{1}{h_1} \right) \qquad (1a)$$

$$t_2 = 61.17 + 1112 \quad 0.00012 + \frac{1}{305} = 64.95°F$$

The thermocouple read 69.47°F (Table C-1, Col. (6)) and the thermal conductance for the attachment of this device, h_{att} 5.6, is found from:

$$h_{att} = \phi_2/(t_{read} - t_2) \qquad (2)$$

$$h_{att}\ 5.6 = 1016/(69.47 - 64.95) = 225\ Btu/hr\text{-}ft^2\text{-}°F$$

Note that the outside surface heat flux ϕ_2 is used in the latter equation. The thermal conductances for the thermocouples at positions 5.6, 6.6, 7.6, and 8.6 were determined by this method for each of the seven all-liquid-inlet tests of run 6. Table 3 shows the mean value and the standard deviation of the individual entries for each thermocouple. The mean value may now be used in conjunction with the observed value of temperature for each thermocouple (from Table C-1) to determine the local film coefficient h_1 (based on one-dimensional theory) for flow at that station. For example, consider the measurement at station 5.6 of test 9 in run 6, which is a two-phase case (x = 12.2%) with ϕ_2 = 1068 Btu/hr-ft^2. The temperature measured by the thermocouple is 77.18°F; the associated h_{att} is 245 Btu/hr-ft^2-°F (Table 3). The tube surface temperature therefore can be calculated by solving Eq. (2) for t_2 as follows:

$$t_2 = t_{read} - \phi_2/h_{att} \qquad (2a)$$

$$= 77.18 - 1068/244 = 77.18 - 4.38 = 72.80°F$$

With the calculated outer wall surface temperature, the approximate liquid local bulk temperature (69.63), and the applicable physical and geometric parameters of the tube, eq. (1) may be used to calculate the two-phase film heat transfer coefficient:

$$\frac{1}{h_1} = \frac{72.80 - 69.63}{1169} - 0.00012$$

$$h_1 = 386\ Btu/hr\text{-}ft^2\text{-}°F$$

The above method was used to determine the heat transfer coefficients for all of the tests, which are shown in Table 4, generally rounded off to two significant figures. These results are discussed in the following sections.

4.3 All-Liquid-Inlet-Flow Heat Transfer

The results obtained from tests 2-7 and 17 of run 6, in which the steam preheater was not actuated, are compared in Fig. 11 with liquid ammonia heat transfer coefficients computed from the Dittus-Boelter equation (Ref. 9),

$$h_L = 0.023 \frac{k}{D_1} Re^{0.8} Pr^{0.4} \qquad (3)$$

which was used in the former analytical predictions (Ref. 1). For these tests, $D_1 = 0.23$ ft, and $k = 0.30$ Btu/hr-ft-°F, $\rho_L = 38.0$ lbm/ft^3, $\mu_L = 0.359$ lbm/hr-ft, and $c_p = 1.15$ Btu/lb-°F (Ref.8), so that

$$h_L = 0.193 V_L^{0.8}$$

This equation is plotted as the curve in Fig. 11. The experimental points in Fig. 11 represent the tube-bottom flow only (6 o'clock position) and are derived from the average of the measurements of the three peened-in thermocouples together with the linearly interpolated bulk temperature at that station. The differences from the Dittus-Boelter equation may be explained by the occurrence of a small amount of nucleate boiling in each of the tests.

During tests 2 through 7, the demister inlet pressure for each succeeding test was adjusted upward with the intention of providing sufficiently subcooled liquid flow to preclude nucleate boiling. However, the measured bulk temperature rise ($\Delta T_{bulk} = T_3 - T_2$) in each case was less than should have resulted as a sensible heat gain for that heating rate with no boiling. The quality x (%) leaving the test section was deduced from

$$Q = \phi_1 A_1 = \dot{w}(c_p \Delta T_{bulk} + \frac{x}{100} i_g), \qquad (4)$$

or

$$x = 100 \left(\frac{\phi_1 A_1}{\dot{w}} - c_p \Delta T_{bulk} \right) / i_g = 2.76 \frac{\phi_1}{\dot{w}} - 0.226 \Delta T_{bulk}$$

where $A_1 = 14.01$ ft^2, i_g = latent heat of vaporization = 508 Btu/lbm, and $\dot{w}$ is in lbm/hr.

Table 4. Deduced Heat Transfer Coefficients

Run/ α(°)/ Test No.	h_1, Btu/hr-ft²-°F																3/4 Tube Avg $h_{1(4)}$	3/4 Tube Avg $h_{1(3)}$	Qual x (%)	V_L (ft/hr)	ϕ_1 Btu/hr-ft²
	TC 5.6	TP 5.3	TP 5.9	TP 5.12	TC 6.6	TP 6.9	TP 6.12	TC 7.6	TP 7.3	TP 7.9	TP 7.12	TC 8.6	TC Avg[c] 18.5.6	TP 8.3	TP 8.9	TP 8.12					
2/+.26/1	2300[a]	2200	2000	71	1000	330	60	760	280	240	53	400	---	440	410	82	575	760	2.7	2230	1193
3/+.26/1	1360	630	520	63	700	630	84	460	530	490	117	330	---	340	350	b	540	576	0[c]	2319	1139
2	b	b	b	90	1680	600	68	1660	480	290	58	990	---	b	220	54	790	1050	4.7	2198	1125
3	b	b	b	97	2300	1140	72	1130	420	390	61	1080	---	b	162	54	806	1070	7.2	2216	1156
4	b	1230	1020	69	b	570	70	b	7800	550	69	b	---	b	620	71	885	1180	19.9	2216	1154
5	b	1280	750	65	5100	360	55	790	650	730	122	480	---	750	400	158	639	1835	0	3527	1144
6	b	b	b	89	b	b	140	14000	930	b	82	2800	---	b	570	72	1030	1360	14.8	3329	1152
4/-.21/1	320	310	330	620	350	325	670	280	300	310	1220	280	---	290	300	2800	474	281	0	2319	1209
2	5100	2100	b	116	1560	b	178	1310	99000	15000	b	1070	---	800	3500	840	1190	1380	9.2	4437	1201
5/-.21/1	b	b	b	b	b	4500	b	1070	1120	1000	1810	820	---	1060	670	1030	1250	1200	0	5910	1161
2	b	b	b	290	b	b	210	40000	b	b	1250	1930	---	1260	3400	1220	1280	1480	7.7	5044	1188
3	b	b	b	122	b	b	145	1790	b	b	770	1220	---	950	8900	770	1170	1430	8.4	5023	2314
4	b	b	b	157	480	580	136	12000	b	b	200	1530	---	1150	b	860	1040	1290	8.9	5037	1192
6/-2.0/8	410	1180	1260	960	440	1450	990	440	1130	1360	670	430	410[c]	290	830	630	831	838	5.5	2146	1169
9	390	820	840	640	390	710	800	440	1080	1130	530	400	410	210	920	530	655	665	12.2	2136	1169
10	530	480	440	62	450	b	390	440	1410	1260	630	470	510	300	1520	600	697	797	18.1	2134	1169
11	670	810	870	570	630	980	720	640	800	790	520	670	590	580	940	610	720	761	3.0	6313	1169
12	1060	1530	2040	420	860	1950	1340	860	1270	1130	470	760	750	600	1130	530	994	1110	6.2	6418	1169
13	1230	1230	1830	196	840	1170	790	910	1600	1440	590	710	720	520	1120	580	967	1130	9.7	6402	1169
14	820	910	1070	138	680	1150	530	760	1470	1310	550	660	670	480	1180	580	819	953	11.2	4248	1169
15	760	1260	1240	186	680	1170	1140	670	1500	1190	450	590	670	410	1230	580	871	974	9.3	4239	1169
16	920	4000	7200	260	1290	b	8200	690	1970	1430	570	660	630	470	2000	630	1060	1180	8.1	4225	2170

[a] Averages are based on replacing all h's having a value greater than 1500 with a value of 1500.
[b] For these entries, deduced outside wall temperature was less than the interpolated local bulk temperature, indicating a high but undeterminable h, so a value of 1500 was assumed and used in the averaging process. (See discussion in Appendix C.)
[c] Average for the peered-in-thermocouples 18.5-in. upstream of exit plane.

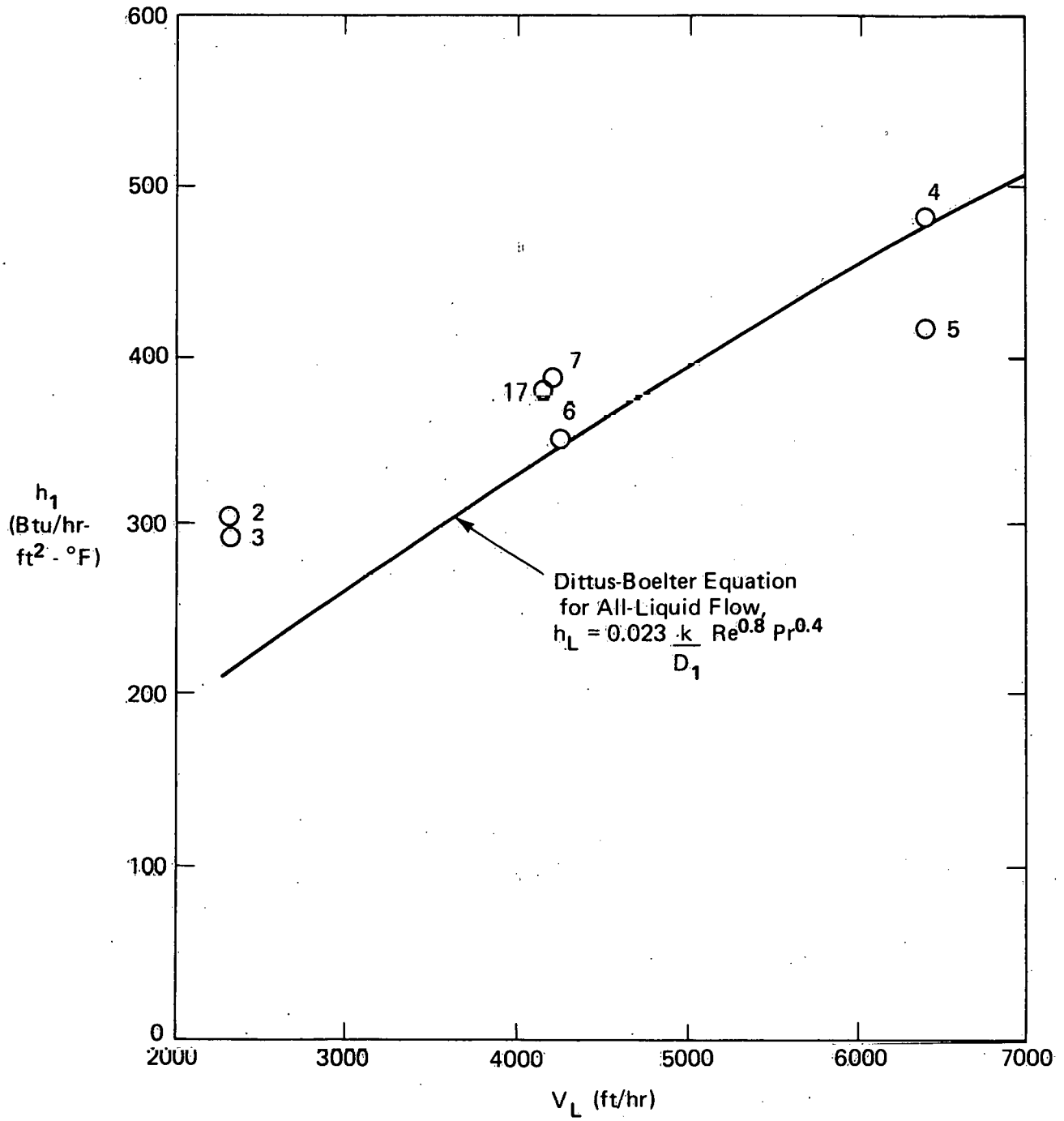

Fig. 11 Comparison of Experimental Heat Transfer Coefficients from the All-Liquid-Inlet Tests of Run 6 with Those Given by the Dittus-Boelter Equation. Test Numbers Appear Adjacent Corresponding Experimental Test Point.

The results are presented in Table 5. The deduced qualities range up to 0.8%. The higher qualities tend to correspond to the greatest deviation of h from the Dittus-Boelter curve (h_L) value, as indicated by the h_1/h_L ratios. Therefore, it is concluded that (a) small amounts of nucleate boiling did occur, and (b) in their absence, the Dittus-Boelter equation does represent the all-liquid convective heat transfer for this heat exchanger. In the following section on the two-phase flow tests (x = 3-20%), reference of the h_1's to the all-liquid value h_L are based on h_L calculated from the Dittus-Boelter equation.

4.4 Comparison of Two-Phase-Flow Results to Chaddock-Brunemann Equation

The overall tubewise averages of the two-phase-flow heat transfer coefficients are listed in Table 4. The ratio of each $h_{1(4)}$ from run 6 to the corresponding Dittus-Boelter h_L is plotted in Fig. 12. The Chaddock and Brunemann correlating equation (Ref. 10) is

$$h_1/h_L = 1.91 \left[Bo \times 10^4 + 1.5\, X_{tt}^{-2/3} \right]^{0.6} \qquad (5)$$

where X_{tt} is the Martinelli parameter. This equation is shown by the curves for two values on Bo x 10^4 (0.090 and 0.285) which bracket the values for the tests. The experimental points are in satisfactory agreement with the correlating curves, including the h_1/h_L's for qualities below 1% from the all-liquid-inlet tests. The point for test 8 is high, but test 8 is a special case because of the mode of operation when it was obtained: just prior to test 8, the demister inlet pressure had been reduced from 167 psia to 127 psia to avoid overstressing the system, and the ammonia apparently was still boiling rather vigorously, even though the steam-jacketed preheater was not in use.

The measured heat transfer coefficient $[h_{1(4)}]_{meas}$ for each two-phase test in runs 2 through 6 is listed in Table 6 together with corresponding coefficient $(h_1)_{CB}$ calculated from the Chaddock-Brunemann correlation. The agreement for tests from runs 2 through 5 is somewhat poorer than for tests from run 6. All of the tests in runs 2 through 5 involve stratified or intermittent flow, which is presumed to be responsible in part for the poorer agreement. Another contributory factor is as follows: During these tests temperature gradients in the oil/ice bath which housed the thermocouple reference junctions were measured. The temperatures observed (and listed in Table C-1) have been corrected by taking into account the oil/ice bath temperature gradient. However, the temperatures measured in these runs are considered to be less accurate than those measured in run 6, prior to which the oil/ice bath gradient was eliminated.

Table 5. Deduced Qualities for All-Liquid-Inlet Tests of Run 6

Test	ϕ (Btu/hr-ft)	$\dot{w}$ (lbm/hr)	ΔT_{bulk} (°F)	x (%)	h_L (Eq. (3)) (Btu/hr-ft-°F)	h_l/h_L	Bo x 10^4
2	1112	3661	2.68	0.23	216	1.41	0.248
3	2165	3650	3.86	0.81	215	1.35	0.485
4	2165	10040	1.73	0.20	483	1.00	0.176
5	1118	10069	1.28	0.02	484	0.87	0.091
6	1118	6664	1.54	0.12	348	1.01	0.137
7	2170	6638	2.54	0.35	347	1.13	0.267
17	2170	6624	1.88	0.48	346	1.10	0.268

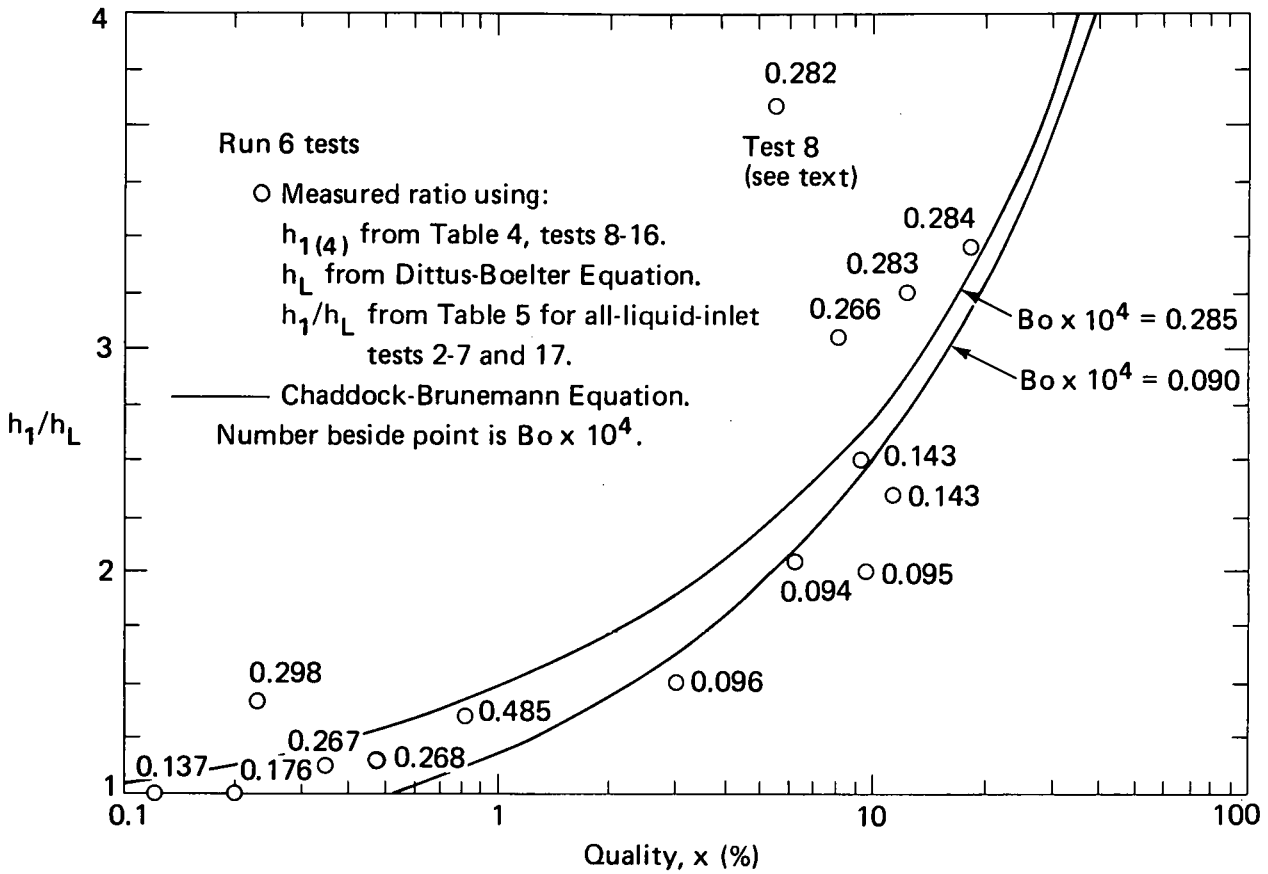

Fig. 12 Comparison of Measured Heat Transfer Coefficients to Chaddock-Brunemann Equation.

Table 6. Measured and Calculated Two-Phase Heat Transfer Coefficients for Runs 2 thru 6

Test/Run		x %	$(h_L)_{DB}$ (Btu/hr-ft^2-°F)	Bo x 10^4	$(h_1)_{CB}$ (Btu/hr-ft^2-°F)	$[h_{1(4)}]_{meas.}$ (Btu/hr-ft^2-°F
6	8	5.5	203	0.282	452	831
	9	12.2	202	0.283	583	655
	10	18.1	202	0.284	675	697
	11	3.0	480	0.096	795	720
	12	6.2	487	0.094	1030	994
	13	9.7	486	0.095	1210	967
	14	11.2	350	0.143	936	819
	15	9.3	349	0.143	872	871
	16	8.1	348	0.266	869	1060
5	2	7.7	401	0.122	928	1280
	3	8.4	400	0.239	1000	1170
	4	8.9	401	0.123	978	1040
4	2	9.2	362	0.140	900	1190
3	2	4.7	207	0.265	437	790
	3	7.2	208	0.270	501	806
	4	19.9	208	0.270	704	885
	6	14.8	288	0.179	866	1030
2	1	2.7	209	0.277	381	575

4.5 Stratified and Intermittent Flow Effects

The experimental data show that stratified or intermittent flow occurs to some degree in all of these low quality ($0.2 \geq x \geq 0.03$), two-phase-flow tests. This effect can be examined partially by considering the circumferential variations in the outside tube wall temperatures (Table 2) and the corresponding heat transfer coefficients (Table 4). When stratified flow occurs, the temperature at the top (12 o'clock position) will be higher, and the heat transfer coefficient will be lower, than those for two-phase or all-liquid flows at the sides and bottom (3, 6, and 9 o'clock) positions. Inspection of the tables indicates that stratified flow occurred at all stations in runs 2 and 3, at stations 5 and 6 in runs 4 and 5, and at station 5 in run 6, tests 10 and 13-16. To assess (with qualifications noted later) the effect of poorer heat transfer at the top of the tube, the ratio of the overall tube average heat transfer coefficient for all four positions, $h_{1(4)}$, to that for the lower 3/4 of the tube (3, 6, and 9 o'clock positions), $h_{1(3)}$, has been listed in Table 7 and plotted in Fig. 13. It is seen that the points from run 6 fall near a value of 0.91; those from runs 4 and 5 near 0.84; and those from runs 2 and 3 near 0.75. The graph at right in Fig. 13 shows the tube declination angle effect.

It should be noted that Fig. 13 does not reflect accurately the effect of stratification on overall heat transfer, because the measurements at the 12 o'clock position do not indicate what is happening at intermediate positions between 12 o'clock and the 3 or 9 o'clock position. (As previously noted, Fig. 12 showed that $h_{1(4)}$'s for run 6 were in good agreement with the Chaddock-Brunemann equation even though Fig. 13 shows that the ratio $h_{1(4)}/h_{1(3)} = 0.91$). This point was supported qualitatively by conducting flow visualization tests in a 3-in.-diameter, 10-ft-long glass tube with mitered glass U-bends at the entrance and exit. Water and air were used to simulate liquid and vapor velocities for an ammonia mass flow of 2.25 lb/sec and a quality of 7.8% at $\alpha = 0$ and $-2°$. Motion pictures of the flow showed that it would be characterized as stratified wavy or intermittent (Ref. 7). The liquid washes up and down the side walls producing thin films (high heat transfer) which periodically cover the tube top as well, even at $\alpha = 0°$. While the situation is better at $\alpha = -2°$ (upward tilt) than at $\alpha = 0°$, it seems reasonable to conclude, noting also the $h_{1(4)}$ values in Table 4 for all runs, that overall internal heat transfer coefficients essentially equivalent to the prior predictions for this heat exchanger concept will be obtained in evaporators using horizontal tubes.

5. CONCLUSIONS AND RECOMMENDATIONS

The results of 29 internal heat transfer tests of an electrically-heated, 3-in.-diameter, 20-ft-long aluminum tube with internal ammonia mass flows of 0.936 to 2.85 lbm/sec, qualities of 0 to 20% (produced by preheating in a steam-jacketed tube), heat fluxes of 1100-2300 Btu/hr-ft^2 and

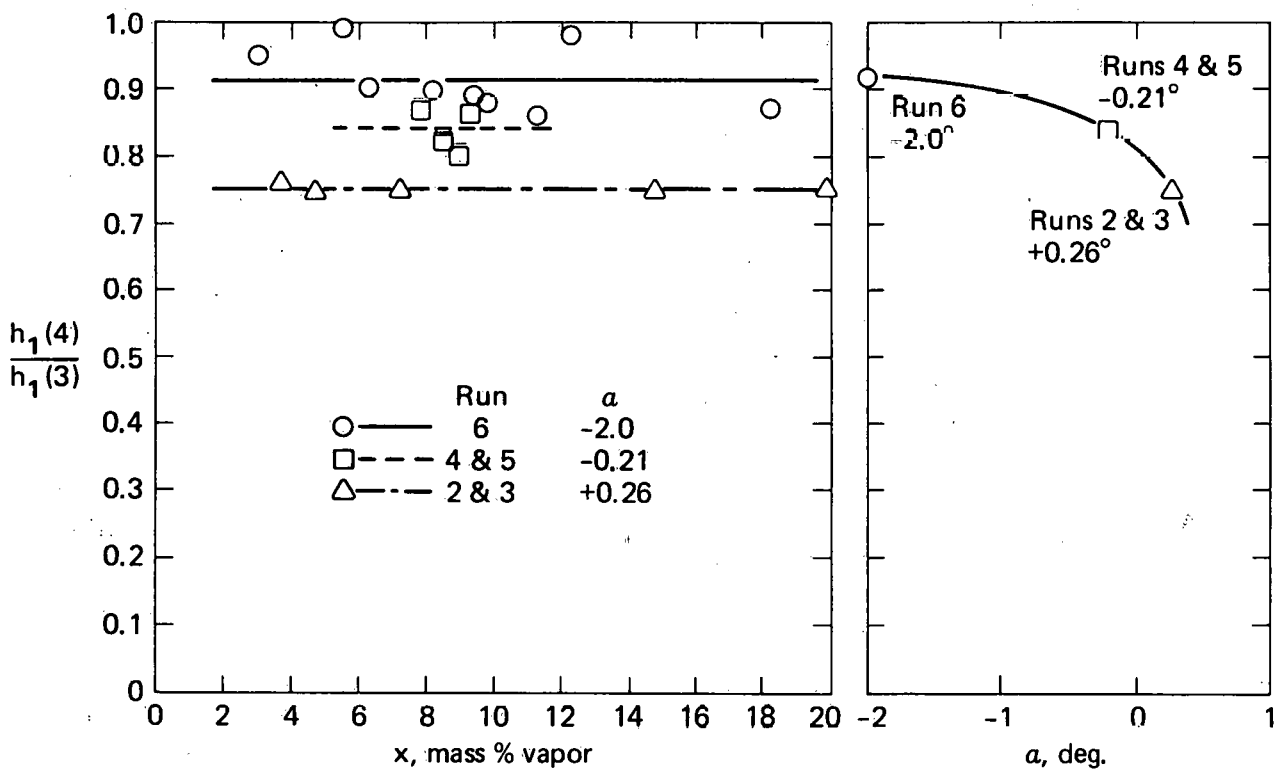

Fig. 13 Effect of Dryout at the Top of the Tube. Ratio of Overall Tube Average Heat Transfer Coefficient to the 3/4-Tube Average is Shown as Functions of Quality x and Declination Angle a.

Table 7 The Effects of Dryout and Tube Inclination Angle on Heat Transfer

Run/ Test	x (%)	$h_{l(3)}$ (Btu/hr-ft^2-°F)	$h_{l(4)}$ (Btu/hr-ft^2-°F)	$\frac{h_{l(4)}}{h_{l(3)}}$	α (deg.)
6- 8	5.5	838	831	0.99	-2.0
9	12.2	665	655	0.98	
10	18.1	797	697	0.87	
11	3.0	761	720	0.95	
12	6.2	1110	994	0.90	
13	9.7	1130	967	0.88	
14	11.2	953	819	0.86	
15	9.3	974	871	0.89	
16	8.1	1180	1060	0.90	
5- 2	7.7	1480	1280	0.87	-0.21
3	8.4	1430	1170	0.82	
4	8.9	1300	1040	0.80	
4- 2	9.2	1380	1190	0.86	-0.21
3- 2	4.7	1050	790	0.75	+0.26
3	7.2	1070	806	0.75	
4	19.9	1180	885	0.75	
6	14.8	1360	1025	0.75	
2- 1	2.7	760	575	0.76	+0.26

declination angles* of + .26° to - 2.0° are summarized as follows:

(a) The Chaddock and Brunemann correlation (Ref. 10) predicts the two-phase heat transfer coefficients for ammonia with acceptable precision for the final run encompassing 16 tests at α = -2.0°, for which the instrumentation was best.

(b) Stratification or intermittent flow to some degree exists at all the tested tube angles. However, its occurrence does not reduce the overall tube heat transfer greatly.

(c) The results of the all-liquid-inlet tests (with no preheating) in the final run suggest that nucleate boiling occurs at the moderate flow rates and heat fluxes tested.

The series of tests conducted represent a progressive learning experience in the handling and expected behavior of ammonia flowing through a large diameter pipe. Instrumentation mounting procedures which were not initially used (i.e., peening of thermocouples to the relatively thin tube wall) because of safety precautions were found to be feasible and were incorporated in the last set of tests; three downstream stations were instrumented with peened-in thermocouples for this final series. As a result, the confidence in the data from the last series of tests (the 16 tests of run 6) is much higher than those of the preceding series, and the foregoing conclusions are based largely upon that last test series.

The foregoing results and conclusions lead to the following recommendations:

(a) The Phase II test program with full-scale models of evaporator and condenser sections in a closed loop ("core tests" in ERDA parlance) should be pursued on a high priority basis.

(b) The stratification flow phenomena should be characterized in more detailed tests at design and off-design operating conditions. This can be done with the existing internal-flow test apparatus but will require replacing some instrumentation: all surface temperature sensors should be replaced with peened-in thermocouples.

(c) The occurrence of nucleation in the sub-cooled flow should be characterized in more detail, especially with respect to the location of inception. This will require additional instrumentation at points between the four stations used in the present series of tests.

*Positive values indicate the downward flow direction (declinations). This convention follows that of Ref. 7.

6. ACKNOWLEDGMENT

The authors gratefully acknowledge the cooperation of their colleagues in the planning and execution of this experiment. Dr. W.H. Avery, Dr. G.L. Dugger, Mr. R.A. Makofski, and Mr. W.B. Shippen provided general guidance, technical input and evaluation and report editing, and correlation with other aspects of the OTEC program. Dr. Peter Griffith of MIT, consultant to APL, provided much helpful advice. Mr. J.L. Keirsey contributed to all aspects of the project and took an active part in the construction and operation of the test loop. Mr. R.T. Cusick designed the instrument complement of the test loop and Mr. M.E. Rose supervised its implementation. The test section instrumentation was installed by Mr. J.E. Creeden. Mr. M. Shandor correlated the test-loop operation with the PRL test facility. The test loop and its components were designed by Mr. A.S. Polk, Jr. and Mr. R.F. Wolff.

We also acknowledge with gratitude the sponsorship of the work by the Solar Energy Division of ERDA, the support provided by Dr. Robert Cohen and Dr. Sigmund Gronich, and the helpful critiques given by Professor Kenneth Bell, Oklahoma State University, Dr. Richard Lyon, ERDA/ORNL, and Professor J.G. Knudsen, Oregon State University.

7. REFERENCES

1. Olsen, H.L. and Pandolfini, P.P., "Analytical Study of Two-Phase-Flow Heat Exchangers for OTEC Systems," APL/JHU AEO-75-37, November 1975, prepared for the Division of Solar Energy, U.S. Energy Research and Development Administration.

2. Olsen, H.L., Pandolfini, P.P., Blevins, R.W., and Avery, W.H., "Design of Low-Cost Aluminum Heat Exchangers for OTEC Plant-Ships," Proceedings of Joint ISES/SESC Conference, Sharing the Sun! Solar Energy in the Seventies, August 15th-20th, 1976, Winnipeg, Vol. 5, Solar Thermal and Ocean Thermal, American Section, Int'l. Solar Energy Soc., Cape Canaveral, Fla., pp. 485-506.

3. Avery, W.H., Blevins, R.W., Dugger, G.L. and Francis, E.J., "Maritime and Construction Aspects of Ocean Thermal Energy Conversion (OTEC) Plant Ships," APL/JHU SR-76-1B, April 1976, prepared for the U.S. Maritime Administration, Department of Commerce.

4. Dugger, G.L., Olsen, H.L., Shippen, W.B., Francis, E.J., and Avery, W.H., "Tropical Ocean Thermal Powerplants and Potential Products," AIAA Paper 75-617, AIAA/AAS Solar Energy for Earch Conference, Los Angeles, Calif., April 21-24, 1975.

5. Dugger, G.L., Olsen, H.L., Shippen, W.B., Francis, E.J., and Avery, W.H., "Floating Ocean Thermal Power Plants and Potential Products," Journal of Hydronautics, October 1975.

6. Dugger, G.L., Francis, E.J., and Avery, W.H., "Technical and Economic Feasibility of Ocean Thermal Energy Conversion," APL/JHU AEO-76-060, August 1976; also in Proceedings of Joint ISES/SESC Conference, Sharing the Sun! Solar Energy in the Seventies, August 15th-20th, 1976, Winnipeg, Vol. 5, Solar Thermal and Ocean Thermal, American Section, Int'l. Solar Energy Soc., Cape Canaveral, Fla., pp. 9-45.

7. Taitel, Y. and Dukler, A.E., "A Model for Predicting Flow Regime Transition in Horizontal and Near Horizontal Gas-Liquid Flow," A.I.Ch.E. Journal, Vol. 22, No.1, Jan. 1976, pp. 47-55.

8. Handbook of Fundamentals, Amer. Soc. of Heating, Refrigeration and Air-Conditioning Engineers (ASHRAE) (New York) 1972.

9. McAdams, W.H., Heat Transmission, 2nd Ed., McGraw-Hill (New York), 1942, p. 148.

10. Pujol, L. and Stenning, A.H., "Effect of Flow Direction on the Boiling Heat Transfer Coefficient in Vertical Tubes," from Cocurrent Gas-Liquid Flow, Rhodes and Scott, Plenum Press, New York, 1969. (Includes Chaddock-Brunneman correlation as used in this report.)

11. Perry's Chemical Engineers' Handbook, 4th Ed., R.H. Perry, C.H. Chilton, and S.D. Kirkpatrick, editors, McGraw-Hill, 1963, p. 3-199.

12. Eckert, E.R.G. and Drake, R.M., Heat and Mass Transfer, 2nd Edition, McGraw-Hill, New York (1959).

13. Chen, J.C., "A Correlation for Boiling Heat Transfer to Fluids in Convective Flow," ASME Paper No. 63-HT-34 (1963).

APPENDIX A

HEAT TRANSFER ANALYSIS FOR SIZING AMMONIA PREHEATER

Nomenclature

A	inside cross-sectional area (ft^2)
D_1	inside diameter (ft)
F	multiplier for Chen correlation
L	length (ft)
Pr_f, Re_f	Prandtl and Reynolds numbers, respectively
S	multiplier for Chen correlation
X_{tt}	Martinelli parameter, Eq. (A-8)
c_{pf}	specific heat of fluid (Btu/lbm-°F)
g_c	acceleration of gravity (ft/hr^2)
h_c, h_{tp}, h_{NuB}	ammonia-side heat-transfer coefficients for all-liquid and two-phase flows, and for nucleate boiling contribution, respectively (Btu/hr-ft^2-°F)
$\bar{h}_f$	heat transfer coefficient of steam-side condensate film (Btu/hr-ft^2-°F)
i_{fg}	latent heat of vaporization (Btu/lbm)
i_{fg}'	modified i_{fg} for condensing steam, Eq. (A-10)
k_f	thermal conductivity of fluid (Btu/hr-ft-°F)
q	heating rate (Btu/hr)
r_1, r_2	inside and outside radii, respectively (ft)
t_1, t_2	inside and outside surface temperatures, respectively (°F)
$\dot{w}_c$, $\dot{w}_m$	mass flows of condensate and ammonia, respectively (lbm/hr)
x	quality (mass fraction of vapor)

Γ	condensate flow rate per unit length (lbm/hr-ft)
ΔT_{SAT}	wall superheat (°F)
ΔP_{SAT}	difference of wall saturation pressure and stream saturation pressure (lbf/ft^2)
μ_f, μ_g	viscosities of liquid and gas, respectively (lbm/hr-ft)
ρ_f, ρ_g, ρ_s	densities of liquid, gas, and metal, respectively (lbm/ft^3)
σ	surface tension (lbf/ft)

Analysis to Determine Preheater Length

In the OTEC internal flow experiment, the steam-jacketed preheater has been designed to deliver to the test section ammonia in two-phase flow at a nominal temperature of 70°F, with qualities as low as 2% for a flow rate of 0.7 lbm/sec, and as high as 20% for 1.5 lbm/sec (or 10% for 3 lbm/sec). The 3-inch, Type 304 stainless steel, schedule 80 pipe has the following properties:

$$O.D. \equiv D_2 \ (= 3.5 \text{ in.}) = 0.2917 \text{ ft}; \ r_2 = 0.1459 \text{ ft}$$

$$I.D. \equiv D_1 \ (= 2.9 \text{ in.}) = 0.2417 \text{ ft}; \ r_1 = 0.1209 \text{ ft}; \ A = \pi r_1^2 = 0.04588 \text{ ft}^2$$

$$k = 9.4 \text{ Btu/hr-ft-°F}; \ \rho_s = 489.3 \text{ lbm/ft}^3$$

The length of pipe needed was determined as follows. The preheater comprises a warm-up section and a two-phase section. In each section the outside wall temperature of the pipe t_2 (at radius r_2 above) is held constant by the steam bath. The inside wall temperature is t_1 (at radius r_1 above). The heat transferred by conduction through the pipe walls is given by the cylindrical steady-state conduction equation

$$(q/L)_S = 2\,k(t_1-t_2)/\ln\,(r_2/r_1) = 314.11\,(t_1-t_2) \text{ Btu/hr-ft} \qquad (A\text{-}1)$$

The heat transfer to the ammonia by convection is

$$(q/L)_A = h\pi D_1(t_{NH_3} - t_1) = 0.7593\,h(t_{NH_3} - t_1) \qquad (A\text{-}2)$$

The preheater is supplied with nominally 65°F subcooled ammonia which is to be heated to nominal 70°F saturated ammonia. The average liquid

temperature in the warm-up section is taken as $t_{NH_3} = 67.5°F$. For the two-phase section $t_{NH_3} = 70°F$. Thus for the warm-up section Eq. (A-2) becomes

$$(q/L)_A = 0.7593\ h_c\ (67.5 - t_l) \tag{A-3a}$$

and for the two-phase section

$$(q/L)_A = 0.7593\ h_{tp}\ (70 - t_l) \tag{A-3b}$$

The heat transfer coefficient h_c for Eq. (A-3a) is given by the Dittus-Boelter equation,

$$h_c = 0.023\ (k_f/D_l)\ Re^{0.8} Pr^{0.4}\ \text{Btu/hr-ft}^2\text{-°F} \tag{A-4}$$

For the two-phase section, the heat transfer coefficient is computed as

$$h_{tp} = h_c F + h_{NuB} \tag{A-5}$$

where

$$h_{NuB} = 0.00122 \left[\frac{k_f^{0.79} c_{pf}^{0.45} \rho_f^{0.49}}{\sigma^{0.5} (\mu_f/g_c)^{0.29} i_{fg}^{0.24} \rho_g^{0.24}} \right] S\ (\Delta T_{SAT})^{0.24} (\Delta P_{SAT})^{0.75} \tag{A-6}$$

and F and S are given by the Chen correlation (Ref. 13). Saturated ammonia at 70°F has the following properties:

$k_f = 0.30$ Btu/hr-ft-°F $c_{pf} = 1.148$ Btu/lbm-°F

$\rho_f = 38.0$ lbm/ft^3 $\rho_g = 0.4325$ lbm/ft^3

$\sigma = 1.445 \times 10^{-3}$ lbf/ft $\mu_f = 0.359$ lbm/hr-ft

$i_{fg} = 508.6$ Btu/lbm $g_c = 4.17 \times 10^8$ ft/hr^2

Thus, Eq. (A-6) becomes

$$h_{NuB} = 9.141\ S\ (\Delta T_{SAT})^{0.24}\ (\Delta P_{SAT})^{0.75} \tag{A-7}$$

The preheater is to produce 20% quality at $\dot{w}_m = 5400$ lbm/hr (1.5 lbm/sec) using enough steam to keep the outside wall at 300°F. At

this ammonia flow rate

$$Re_f = \frac{\dot{w}\, D_1}{A\, \mu_f} = \frac{5400(0.2417)}{0.04588(0.359)} = 79240$$

$$Pr_f = c_{pf}\, \mu_f / k = 1.148(0.359)/0.30 = 1.374$$

and, per Eq. (A-4), for the warm-up section,

$$h_c = 269 \text{ Btu/hr-ft}^2\text{-°F}$$

In the steady state, $(q/L)_A$ per Eq. (A-1) must equal $(q/L)_S$ per Eq. (A-3a); solving this equality for t_1 yields

$$t_1 = 208.4 \text{ °F}$$

and substituting this in Eq. (A-1) yields

$$(q/L)_A = 28800 \text{ Btu/hr-ft}$$

where

$$q = \dot{w}_m\, c_p\, \Delta T = 5400(1.148)(5) = 31000 \text{ Btu/hr}$$

hence

$$L_{\text{warm-up}} = 31000/28800 = 1.08 \text{ ft}$$

For the two-phase section, calculations are made for 0.05 increments in quality x. The Martinelli parameter is given by:

$$\frac{1}{X_{tt}} = \left(\frac{x}{1-x}\right)^{0.9} \left(\frac{\rho_f}{\rho_g}\right)^{0.5} \left(\frac{\mu_g}{\mu_f}\right)^{0.1} \qquad \text{(A-8)}$$

which for these ammonia properties reduces to:

$$\frac{1}{X_{tt}} = \left(\frac{x}{1-x}\right)^{0.9} \left(\frac{38}{0.4325}\right)^{0.5} \left(\frac{0.0239}{0.359}\right)^{0.1} = 7.148 \left(\frac{x}{1-x}\right)^{0.9}$$

Equations (A-1) and (A-3b) are solved simultaneously to find the length required for each 0.05 increment in quality. The parameters needed for Eq. (A-3b) (see Ref. 13) are as follows:

x	$\frac{1}{X_{tt}}$	F	$h_c F$	$Re_f F^{1.25}$	S	9.141S
0.05	0.505	1.70	457	153800	0.275	2.514
0.10	0.989	2.67	718	270400	0.156	1.426
0.15	1.500	3.32	893	355100	0.155	1.051
0.20	2.053	4.37	1176	500700	0.095	0.868

The design is done for an outside wall temperature $t_2 = 300°F$ in Eq. (A-1) for the steam side and an ammonia saturation temperature $t_{NH_3} = 70°F$ in Eq. (A-3b). For x = 0.05, Eq. (A-3b) becomes

$$(q/L)_A = 0.7593 \left[457 + 2.514 \, (\Delta T_{SAT})^{0.24} (\Delta P_{SAT})^{0.75} \right] (70 - t_1).$$

Equations (A-1) and (A-3b) must be solved simultaneously by bracketing guesses on t_1 and linear interpolation, since $(\Delta T_{SAT}) = (t_1 - 70)$ and $(\Delta P_{SAT}) = P_{SAT}(t_1) - P_{SAT}(70)$:

Guess $t_1 = 88°F$. This yields $(q/L)_S = 66600$, and

$$(q/L)_A = 0.759 \left\{ 457 + 2.514 \, (18)^{0.24} \left[(174.8 - 128.8) \, 144 \right]^{0.75} \right\} (18) = 56700$$

Guess $t_1 = 90°F$. This yields $(q/L)_S = 66000$ and

$$(q/L)_A = 0.7593 \left\{ 457 + 2.514 \, (20)^{0.24} \left[(180.6 - 128.8) \, 144 \right]^{0.75} \right\} (20) = 69800$$

Graphical interpolation (Fig. A-1) yields $t_1 = 89.5°F$. Then Eq. (A-1) gives

$$(q/L)_S = 314.1 \, (89.5 - 300) = 66100 \text{ Btu/hr-ft}$$

where

$$q = x \, i_{fg} \, \dot{w}_m = 0.05(508.6)(5400) = 137300 \text{ Btu/hr}$$

hence

$$L_{x = 0 - 0.5} = 2.08 \text{ ft}$$

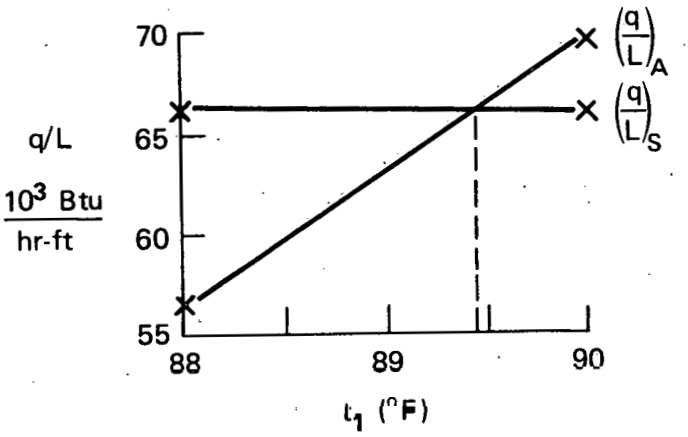

Fig. A-1 Graphical Interpolation to Find t_1 and q/L.

Similar calculations are made for x = 0.10, 0.15, and 0.20, using the proper values of $h_c F$ and 9.141 S in Eq. (A-3b). The results, for t_2 = 300°F and $\dot{w}_m$ = 5400 lbm/hr (1.5 lbm/sec), are summarized below:

Section	x	h (Btu/hr-ft²-°F)	t_1 (°F)	L (ft)
Warm-up	0	269	208.4	1.08
1	0.05	4455	89.5	2.08
2	0.10	3601	93.7	2.12
3	0.15	3218	96.2	2.15
4	0.20	3150	96.7	2.15
		Total preheater length=		9.58

Off-design Performance

The preheater is also intended to deliver saturated ammonia at 70°F at a quality as low as 2% and at a flow rate of 2500 lbm/hr (0.7 lbm/sec). The two-phase section of the preheater to do this must be long enough so that, with a variation in the steam temperature, it may be calibrated to produce this lower demand. Therefore, a computation is done with a 212°F outside wall temperature.

For the warm-up section, the Re_f is 37,000 and h_c is 146 Btu/hr-ft²-°F. In the steady state, equating Eqs. (A-1) and (A-3a)

yields t_1 = 174.3°F, and $(q/L)_A$ = 11856 Btu/hr-ft, where q = 14465 Btu/hr, so that L = 1.22 ft.

For the two-phase section to provide 0.02 quality, X_{tt}^{-1} = 0.215, F = 120, S = 0.573. Simultaneous solution of Eqs. (A-1) and (A-3b) using graphical interpolation similar to Fig. A-1 yields t_1 = 81.2°F, $(q/L)_S$ = 41100 Btu/hr-ft, q = 25600, and hence L = 0.62 ft. Thus the total length needed, including 1.22 ft for the warm-up section, with t_2 = 212°F, to produce x = 0.02 for a 2500 lbm/hr flow, is 1.84 ft.

Viscosity Uncertainty

The properties of ammonia at 70°F have been used throughout. There is a question about the correct value of the liquid viscosity. However, the variation in preheater tube length required to reach 0.20 quality with 1.5 lbm/sec for three different values of μ_f is very small.

Source	μ_f(lbm/hr-ft)	Length (ft)
Chemical Engineer's Handbook (Ref. 11)	0.269	9.54
ASHRAE Handbook (Ref. 8)	0.359*	9.58
Eckert and Drake (Ref. 12)	0.528	9.60

*This value used in Ref. 1 and in present report.

Required Steam Temperature

The steam supply temperature must be higher than the outer surface temperature t_2, since a liquid film must be condensing around the pipe. Laminar film condensation on the outside of a horizontal tube was first examined by Nusselt who assumed that temperature drop between the vapor interface and tube wall is constant. The equations that apply are as follows:

$$\bar{h}_f = 0.725 \left[\frac{\rho_f(\rho_f - \rho_g) g_c \, i_{fg}' \, k_f^3}{D_2 \, \mu_f \, (\Delta T_f)} \right]^{\frac{1}{4}} \qquad \text{(A-9)}$$

$$i_{fg}' = i_{fg} \left(1 + 0.68 \, \frac{c_{pf} \, \Delta T_f}{i_{fg}} \right) \qquad \text{(A-10)}$$

$$\frac{\bar{h}_f}{k_f} \left[\frac{\mu_f^2}{\rho_f(\rho_f - \rho_g) g_c} \right]^{\frac{1}{3}} = 1.51 \, Re_T^{-\frac{1}{3}} \qquad \text{(A-11)}$$

$$Re_T = 4\Gamma/\mu_f = 4\dot{w}_c/L\mu_f \qquad \text{(A-12)}$$

The solution for the design case of a 9.6-ft-long preheater with $t_2 = 300°F$ is that a saturated steam temperature of approximately 350°F is required, determined as follows.

The required heat flow to the ammonia is:

$$q = \dot{w}_m\,(c_p\Delta T + i_{fg}) = 5400\quad (1.148)(5) + 0.2(508.6) \quad = 581{,}000 \text{ Btu/hr}$$

The flow of steam (with a latent heat of 871 Btu/lbm at 300°F) is

$$\dot{w}_c = q/i_{fg} = 581{,}000/871 = 667 \text{ lbm/hr}$$

The Reynolds number for the condensate flow is

$$Re_T = 4\dot{w}_c/L\mu_f = 4(667)/9.6(0.38) = 731$$

Other properties of steam at 350°F needed for Eq. (A-10) are:

$c_{pf} = 1.044$ Btu/lbm-°F

$k_f = 0.391$

$\mu_f = 0.38$ lbm/hr-ft

$\rho_f = 55.59$ lbm/ft^3

$\rho_g = 0.30$ lbm/ft^3

Equation (A-10) yields

$$h_f = 1357 \text{ Btu/hr-ft-°F}$$

Solving Eq. (A-8) for i_{fg}' as a function of ΔT_f yields

$$i_{fg}' = 17.76\,\Delta T_f$$

Equation (A-9) yields another relationship:

$$i_{fg}' = 871 + 0.000815\,\Delta T_f$$

The simultaneous solution of these equations yields

$$\Delta T_f = 49.0°F$$

Thus, to keep the tube outside wall at 300°F, a steam bath of approximately 350°F must be provided.

Similarly, for the off-design low flow case (0.7 lbm/sec, 2% quality), the preceding calculations were repeated, using properties for 212°F steam. The result was a required steam temperature of 226°F.

Summary

These calculations indicate that a 9.6-ft-long preheater would be adequate for the design condition (1.5 lbm/sec, 0.20 quality). The minimum length needed for 0.7 lbm/sec at 0.02 quality is 1.9 ft. To be conservative and to provide a digital approach to steam preheating variation, it was decided to use a total of four steam jackets, one each of 1-ft and 2-ft length and two of 4-ft length, for a maximum combined length (all the same pipe) of 11 ft.

Steam temperatures between 226°F and 350°F must be used in order to provide wall temperatures between 212°F and 300°F. Since steam up to 400°F is available at the test facility, there is no difficulty in maintaining the desired conditions.

APPENDIX B

DESIGN OF THE DEMISTER AND SUMP

B.1 Demister Design

The ammonia demister (Fig. B.1) was procured from York Separators, Inc., Parsippany, N.J., to meet the following specifications:

Operating Conditions:

Flow rate range:	0.7 - 1.5 lb/sec
Quality range:	0.25 mass % vapor
Maximum pressure:	200 psia; maximum temperature: 100°F
Liquid density:	39 lb/ft^3; vapor density: 0.43 lb/ft^3
Maximum velocity of two-phase flow:	30 ft/sec in 3-in. tube

External Connections:

3-in., flanged, for side entry, top outlet, and drain bottom; 3/4 pipe coupling for vent at side

Demisting requirement:

Eliminate 100% of mist particles $\geq$ 5 μm size

Materials and Cleaning:

Carbon steel container; stainless steel wire mesh filter. Prime coat outside; inside furnished as rust- and oil-free as possible including washing and drying stainless screen.

No ASME code stamping required.

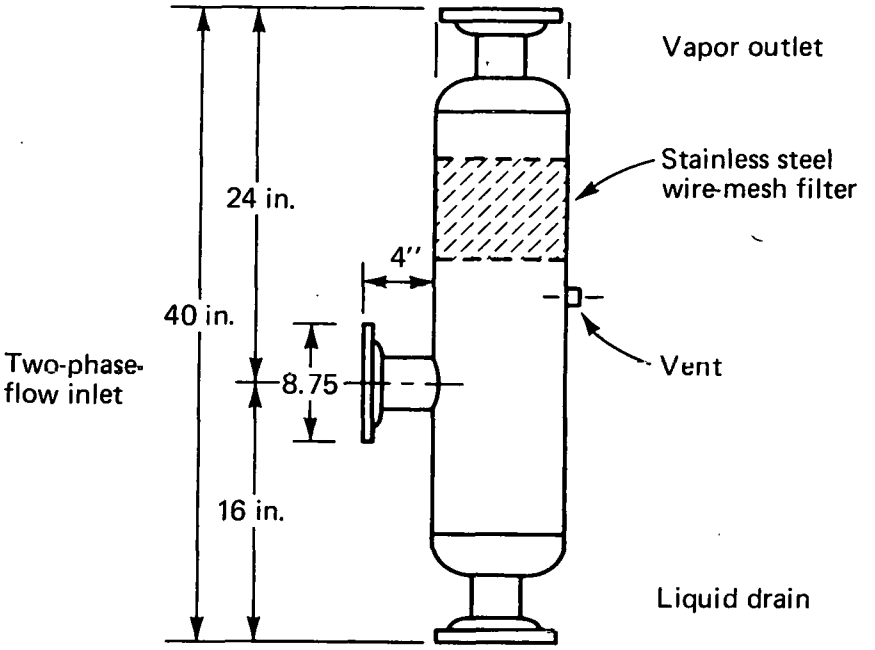

Fig. B-1. The Ammonia Demister.

B.2 Sump Design

The ammonia sump (Fig. B.2) was designed and fabricated at APL/JHU. Its housing is an 8-inch carbon steel pipe (8.625 O.D. x 0.277 wall) with a 150-lb carbon steel slip-on flange at the top, and a 7/8-in. thick base plate at the bottom. The base plate has a 1/2-in. drain line at center and four threaded rods as adjustable support feet. A 2-in., schedule 40, 304 stainless steel outlet with a 2-in., 150-lb carbon steel slip-on flange is provided 4.062 in. from the bottom for attachment to the pump inlet. Total height of the sump housing is 5 ft 4.875 in. A cap plate at the top includes the penetration into the sump for ammonia make-up flow, a pressure tap, a nitrogen pressurization tap, a vacuum line and one additional tap. The vapor cavity in the top of the sump is connected to the demister vapor through a 3/8-in. pipe.

Liquid ammonia is admitted from both the demister and the make-up flow through a single 3-in., schedule 10, 304 stainless steel pipe entering at the top of the sump, along the sump vertical centerline. The pipe is sized for low ammonia velocity to avoid significant entrainment of bubbles into the sump. The bottom end of the vertical pipe is closed off, and the ammonia is discharged in small horizontal jets into the sump proper, through 112, 1/4-in.-diameter holes equally spaced around the pipe circumference, in seven vertical rows.

The level of liquid ammonia in the sump is controlled to provide the required constant 4-ft positive suction head above the pump inlet by continually admitting make-up ammonia to replace the ammonia vapor that is constantly being discharged from the test apparatus during a test. The liquid level is sensed by a variable-capacitance probe (Fig. B.3) whose electrical output signal (1-5 milliamps) is proportional to the liquid level. This signal is used through appropriate electro-pneumatic converter circuitry to provide a pneumatic signal to the dome of the control valve to control ammonia make-up flow rate. The liquid level sensor is installed in a 2-in., schedule 40, black iron pipe, which is mounted vertically alongside the sump housing, and connected to the sump at the top and bottom with 1/4-in. tubing.

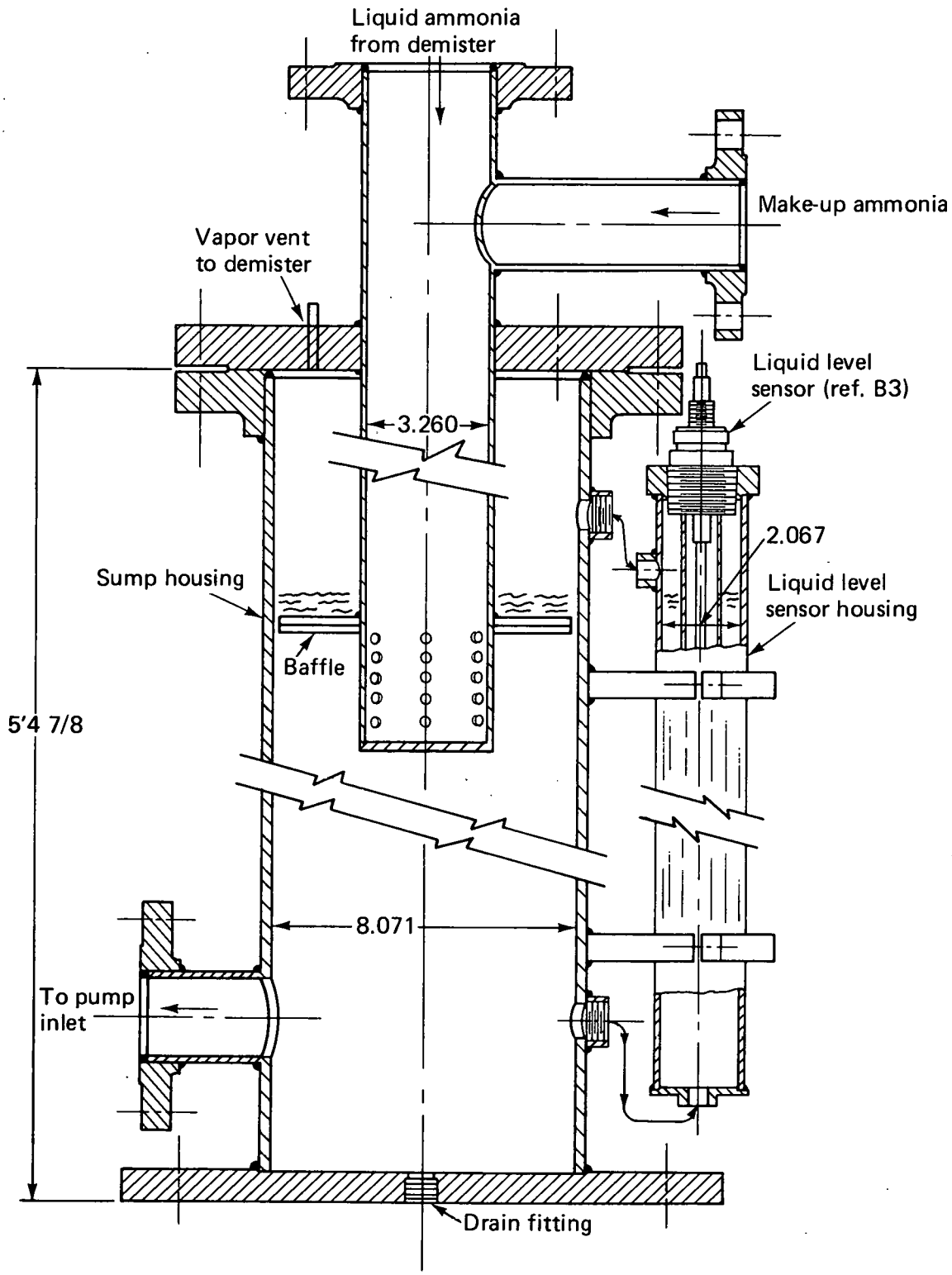

Fig. B-2. The Ammonia Sump, Liquid Ammonia Inlet System, and Ammonia Liquid Level Sensor.

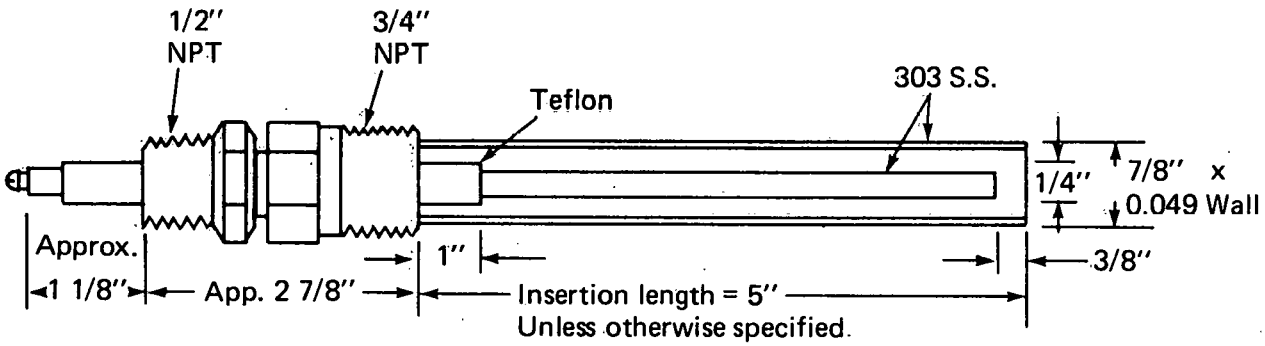

Fig. B-3. Capacitive Probe with Concentric Shield for Sensing the Ammonia Liquid Level in the Sump.

APPENDIX C

REDUCTION OF TEMPERATURE DATA

The voltages sensed by the thermocouples and thermopiles during test runs are converted to digital form by the Digital Data Acquisition and Control System (DIDACS) and stored on a magnetic tape as bit counts. The first step in the data reduction procedure is to obtain a listing of the average points and calibration runs. The data may then be reduced to engineering units as follows:

(1) Convert the bit count reading to a voltage reading by means of the device calibration.

(2) Correct the voltage reading for reference junction deviations.

(3) Convert the voltage into engineering units by means of the standard copper-constantan conversion tables.

To illustrate this data reduction procedure consider the result of run 6, test 2 for TC 5.6. The average bit count for this measurement is 316.75 bits. The calibration to convert this reading to millivolts, taken immediately before the start of run 6, is the following:

$$(mV)_{5.6} = \frac{[(Bits) + 3.56]_{5.6}}{396.67} \qquad (C\text{-}1)$$

$$= \frac{[316.75 + 3.56]}{396.67} = 0.8075 \text{ mV.}$$

The reference junction of TC 5.6 is immersed in an oil bath which, in turn, is immersed in an ice bath. During the run, readings of a thermopile placed between the oil bath and ice bath were also taken. This thermocouple gave an average digital reading of -10.79 bits for the entire run 6; with the calibration of this thermocouple a correction voltage, to be added to the above calculated voltage, is obtained

$$(mV)_{ICE\text{-}OB} = \frac{[(Bits)+15.78]}{396.22} = \frac{[-10.79+15.78]}{396.22} = 0.0126 \text{ mV.} \qquad (C\text{-}2)$$

The corrected voltage reading for TC 5.6 is, therefore, 0.8075 + 0.0126, or 0.8201 mV. From the standard copper-constantan thermocouple tables the corresponding temperature for this voltage is 69.47°F. These temperature readings for thermocouples at positions 5.6, 6.6, 7.6 and 8.6 (prior to the thermal contact resistances described in section 4.2) are shown in Table C-1.

Obtaining the temperature difference reading for a thermopile requires a slightly different procedure:

(1) Convert the bit count reading to a voltage reading by means of the device calibration.

(2) Convert the voltage into engineering units by means of a formula based on standard copper-constantan conversion tables.

To illustrate this procedure consider the result of run 6, test 2 for TP 5.12. The average bit count for this measurement is 91.75 bits. The calibration to convert this reading to millivolts is

$$(\text{mV})_{5.12} = \frac{[(\text{Bits}) + 3.00]_{5.12}}{396.26} = \frac{[91.76 + 3.00]}{396.26} = 0.2391 \text{ mV} \qquad \text{(C-3)}$$

For a four-junction thermopile the conversion formula to engineering units is based upon the standard tables

$$(\Delta°\text{F}) = \frac{40}{1.88 + 0.002T} \quad (\text{mV}) \qquad \text{(C-4)}$$

where (mV) is the value obtained from Eq. (C-3), and T is the nominal temperature at which the measurement is made. For TP 5.12, the nominal temperature is 70°F so,

$$(\Delta°\text{F})_{\text{read } 5.12} = \frac{40}{1.88 + 0.002(70)} \quad (0.2391) = 5.09°\text{F}$$

The method of deducing the thermal conductance coefficients (h_{att}'s) to represent the net effect of thermal contact resistance on the thermopile readings is described as follows:

(1) Each thermopile has two junctions: one is attached at the 6 o'clock position (in proximity to but separate from the thermocouple junction there; see Fig. 10), and the other is attached at either the 3, the 9, or the 12 o'clock position. Each of the two junctions has a thermal contact resistance. The problem is to determine the net difference in resistance between the two, which affects the temperature difference for the outside tube wall between the 6 o'clock position and the position being measured (3, 9, or 12 o'clock).

(2) All-liquid-inlet tests from run 6 are used to determine this net resistance. It is assumed that the true inside surface temperature t_1 is constant around the tube circumference at each station in these all-liquid-inlet tests, and hence the outside wall temperature t_2 is also constant circumferentially.

(3) Referring to the sketch at right*, the temperatures seen by each junction are:

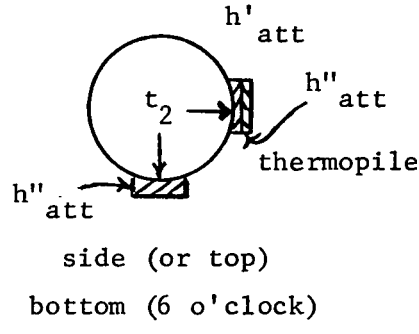

$$t_{TPJ_{3,9,or12}} = t_2 + \phi_2 \left(\frac{1}{h'_{att}} + \frac{1}{h''_{att}} \right)$$

Subtract $$t_{TPJ_6} = t_2 + \phi_2 \left(\frac{1}{h'_{att}} \right)$$

Result = $$\Delta t_{TPJcorr_{3,9,or\ 12}} = \phi_2 \left(\frac{1}{h''_{att}} \right)$$, the deduced temperature difference for the thermopile,

where $\phi_2 = Q/A_2$, the heat flux at the outside surface.

(4) The statistical average h''_{avg} of the seven values of net thermal conductance so deduced from the all-liquid-inlet tests 2-7 and 17 of run 6 is then calculated for each thermopile. It should be noted that the h''_{att} increment of thermal conductance could occur at the 6 o'clock position instead of the 3, 9, or 12 o'clock position, so the foregoing process leads to negative values for some thermopiles. These values are listed in Table C-2. The wall temperature at the thermopile position is calculated as follows:

---

*h'_{att} is the thermal conductance associated with the smaller resistance; h''_{att}, with the additional resistance at the other junction.

$$(\Delta^{\circ}F)_{read_{3,9,or\ 12}} - \frac{\phi_2}{\left(h_{att}''_{avg}\right)_{3,6,or\ 9}} = \Delta t_{2_{3,9,or\ 12}}$$

(Table C-1) (Table C-2)

$$t_{2_{3,9,or\ 12}} = t_{2_6} + \Delta t_{2_{3,9,or\ 12}}$$

(Table 2) (Table 2)

Table C-1. Primary Thermocouple (TC, Temperature) and Thermopile (TP, Temperature Difference) Test Data Reduced to Engineering Units (°F)

(1) Run	α (°)	(2) Test	(3) Qual. x (%)	(4) TC 2	(5) TC 3	(6) TC 5.6	(7) TP 5.3	(8) TP 5.9	(9) TP 5.12	(10) TC 6.6	(11) TP 6.9	(12) TP 6.12	(13) TP 7.6	(14) TP 7.3
2	+0.26	1	2.7	72.66	73.66	77.99	1.35	5.02	18.98	83.11	4.68	17.91	78.23	3.15
3	+0.26	1	0	73.15	74.90	78.75	2.22	6.08	19.79	83.94	2.32	11.35	79.94	0.04
		2	4.7	72.75	74.40	77.14	0.74	4.26	15.31	82.43	3.31	15.21	77.63	2.03
		3	7.2	72.59	74.14	77.32	0.26	4.47	14.58	82.30	2.68	14.89	77.53	2.10
		4	19.9	72.47	80.00	76.06	4.60	8.29	21.80	81.22	7.01	18.75	76.69	4.12
		5	0	73.27	75.13	77.47	2.76	6.86	20.81	82.73	5.09	19.90	79.09	0.70
		6	14.8	72.77	73.43	75.34	1.86	5.68	17.54	80.18	2.63	8.99	76.53	1.54
4	-0.21	1	0	70.56	72.79	79.48	1.40	4.87	0.91	83.94	2.48	-2.37	79.67	0.05
		2	9.2	70.60	70.98	75.57	1.66	4.41	12.83	80.44	1.09	5.34	75.17	-0.50
5	-0.21	1	0	64.73	66.12	68.28	1.48	4.79	3.68	73.88	2.46	-1.72	69.95	0.35
		2	7.7	64.55	64.97	66.65	1.06	4.18	9.32	72.48	1.72	6.09	68.22	-0.26
		3	8.4	64.39	64.69	71.01	3.15	8.26	26.68	81.00	2.87	15.35	72.46	-0.65
		4	8.9	69.15	69.23	70.80	0.97	4.68	13.26	80.53	1.81	5.60	72.70	-0.13
6	-2.0	2	0	60.63	63.31	69.47	1.48	5.10	5.09	73.56	2.80	2.34	69.24	1.11
		3	0	68.51	72.37	85.59	2.30	9.30	3.84	93.95	4.57	5.40	85.28	0.11
		4	0	70.61	72.34	83.63	2.00	8.77	4.72	91.96	4.24	-2.02	82.25	0.34
		5	0	73.41	74.69	81.27	1.60	5.09	4.01	86.52	2.23	-0.50	80.17	0.72
		6	0	79.27	80.81	86.73	1.22	4.64	3.45	91.29	1.70	-0.51	86.34	0.56
		7	0	83.64	86.09	96.97	2.09	8.22	5.26	104.47	3.19	-0.73	96.12	0.53
		17	0	69.96	71.84	84.26	2.28	7.97	2.58	91.84	4.34	-3.47	82.93	- .95
		8	5.5	69.77	69.74	77.12	-0.56	2.93	1.03	81.12	0.32	-2.14	75.73	-1.22
		9	12.2	69.66	69.53	77.18	-0.31	3.20	1.44	81.33	0.81	-2.23	75.57	-1.18
		10	18.1	69.71	69.80	76.45	1.54	5.28	19.45	81.02	-2.78	-0.25	75.74	-1.42
		11	3.0	69.74	69.71	76.00	0.98	4.43	2.95	80.26	1.54	-0.87	74.90	0.01
		12	6.2	69.97	69.73	75.55	0.94	4.30	4.31	79.91	1.44	-1.13	74.53	-0.06
		13	9.7	70.05	69.87	75.49	1.28	4.52	7.65	80.04	1.81	-0.55	74.56	-0.16
		14	11.2	69.82	69.82	75.77	1.14	4.50	9.67	80.21	1.50	-0.16	74.70	-0.36
		15	9.3	69.91	70.08	76.00	0.68	4.24	7.41	80.38	1.47	-1.34	75.09	-0.57
		16	8.1	69.78	69.76	80.55	0.56	6.91	10.87	87.57	2.35	-2.61	79.12	-1.35

Table C-1 (concluded)

Run	α (°)	Test	Qual. x (%)	(15) 7.9	(16) 7.12	(17) 8.6	(18) 8.3	(19) 8.9	(20) 8.12	(21) 17.5.6	(22) 18.5.6	(23) 19.5.6	(24) Q (Watts)
2		1	2.7	2.89	23.17	79.25	-1.16	-0.76	9.56	--	--	--	4897
3		1	0	-0.59	9.46	80.69	-1.22	-0.44	0.86	--	--	--	4678
		2	4.7	2.81	20.84	77.82	-4.32	3.35	17.92	--	--	--	4617
		3	7.2	1.57	20.11	77.59	-4.36	3.20	17.54	--	--	--	4747
		4	19.9	5.30	22.50	76.96	-6.40	5.45	18.53	--	--	--	4737
		5	0	-0.28	10.15	79.31	-1.69	-0.15	2.95	--	--	--	4695
		6	14.8	0.18	16.12	76.39	-2.05	1.00	13.57	--	--	--	4728
4		1	0	-0.84	-1.03	79.45	-0.94	-0.89	-5.90	--	--	--	4964
		2	9.2	-1.26	-5.97	74.81	-0.49	-1.42	-1.70	--	--	--	4932
5		1	0	-0.33	1.77	69.95	-1.15	-0.30	-2.23	--	--	--	4765
		2	7.7	-1.11	3.18	68.26	-0.52	-1.21	-1.62	--	--	--	4877
		3	8.4	-2.77	6.11	71.88	-1.10	-2.86	-2.75	--	--	--	9498
		4	8.9	-1.37	8.10	72.75	-0.59	-1.43	-1.38	--	--	--	4893
6		2	0	0.24	3.62	68.66	-1.40	0.34	-1.26	66.51	67.17	67.09	4563
		3	0	-0.98	0.73	84.38	-1.03	-1.92	-7.33	79.80	79.90	79.79	8890
		4	0	-0.84	3.86	81.46	-1.75	-1.14	-3.97	76.86	77.15	76.85	8890
		5	0	-0.27	3.82	80.14	-0.98	-0.38	-1.46	77.44	77.49	77.26	4588
		6	0	-0.04	3.21	86.48	-0.93	-0.44	-1.63	83.92	84.08	84.02	4588
		7	0	-0.59	4.49	95.60	-1.82	-1.14	-3.42	91.69	91.71	91.79	8907
		17	0	-1.54	1.87	82.22	-1.02	-2.53	-5.51	77.63	77.79	77.60	8907
		8	5.5	-2.20	1.33	75.17	0.46	-1.93	-2.82	72.73	73.03	72.46	4799
		9	12.2	-1.90	1.78	75.17	1.76	-2.25	-2.64	72.53	72.52	72.44	4799
		10	18.1	-2.13	1.44	75.00	0.59	-2.36	-2.50	72.26	72.18	72.22	4799
		11	3.0	-0.78	2.61	74.17	-0.56	-1.12	-1.78	71.81	71.76	71.88	4799
		12	6.2	-0.75	3.34	74.03	-0.42	-1.13	-1.27	71.53	71.46	71.34	4799
		13	9.7	-0.89	2.91	74.27	-0.24	-1.39	-1.51	71.61	71.77	71.58	4799
		14	11.2	-1.07	2.82	74.30	-0.17	-1.40	-1.72	71.58	71.88	71.66	4799
		15	9.3	-1.18	3.09	74.72	0.03	-1.64	-1.91	71.92	72.02	71.91	4799
		16	8.1	-2.43	4.78	78.08	-0.24	-3.36	-3.47	73.75	73.27	73.55	8907

THE JOHNS HOPKINS UNIVERSITY
APPLIED PHYSICS LABORATORY
LAUREL, MARYLAND

Table C-2. Deduced Attachment Conductances for Thermopiles (h''_{att}; See Text)

Test	Sta.5.3	5.9	5.12	6.9	6.12	7.3	7.9	7.12	8.3	8.9	8.12
6/2	690	199	200	360	430[a]	920	4230[a]	280	- 730	3000[a]	- 810
3	860	213	510	430	370[a]	18000[a]	-2020	2710[a]	-1920	-1030	- 270
4	990	226	420	470	- 980	5820	-2360	510	-1130	-1740	- 500
5	640	201	255	460	-2040	1420	-3780	270	-1040	-2690	- 700
6	840	220	296	600	-2000	1820	-25000[a]	320	-1100	-2320	- 630
7	950	241	380	620	-2720	3740	-3360	440	-1090	-1740	- 580
17	870	249	770	460	- 570	-2090[a]	-1290	1060	-1940	- 780	- 360
Avg.	830	221	404	486	-1660	-2740	-2560	480	-1280	-1720	- 550

[a]Ignored in computing the average.

APPENDIX D

SOLUTION OF ONE-DIMENSIONAL STEADY-STATE CYLINDRICAL HEAT CONDUCTION EQUATION

Statement of Problem:

A tube of given length, diameter and wall thickness has a fluid with bulk temperature t_{NH} flowing inside. If Q watts are uniformly put into the tube over its entire length, find the relation between the outer surface wall temperature and the inside heat transfer film coefficient in the steady state.

Nomenclature:

A_2	outer surface area (ft^2)
d_1	inner diameter (in.)
d_2	outer diameter (in.)
h_1	inner wall film heat transfer coefficient (Btu/hr-ft^2-°F)
k	thermal conductivity (Btu/hr-ft-°F)
ℓ	length of tube (in.)
Q	heating power (watts)
t_{NH}	bulk fluid temperature (°F)
t_2	outside wall temperature (°F)

NOTE: 1 watt = 3.413 Btu/hr

One-dimensional steady-state cylindrical conduction equation:

$$\frac{\partial^2 t}{\partial r^2} + \frac{1}{r}\frac{\partial t}{\partial r} = 0 \qquad \text{(D-1)}$$

Solution:

$$t = C_1 \ln r + C_2 \qquad \text{(D-2)}$$

Boundary conditions:

$$@\ r = r_1 = d_1/2$$

$$k\left(\frac{\partial t}{\partial r}\right)_{r=r_1} + h_1 t_1 = h_1 t_{NH_3} \qquad \text{(D-3)}$$

$$@\ r = r_2 = d_2/2$$

$$-k\left(\frac{\partial t}{\partial r}\right)_{r=r_2} = \frac{-3.413\ Q}{A_2} \qquad \text{(D-4)}$$

Evaluation of C_1 and C_2; for d, r, and ℓ inputs in inches:

From Eq. (D-4)

$$\frac{\partial t}{\partial r} = \frac{3.413\ Q}{\pi \frac{d_2}{12} \frac{\ell}{12} k} = \frac{491.472\ Q}{\pi\ d_2\ \ell\ k} \qquad \text{(D-5)}$$

From Eq. (D-2)

$$\frac{\partial t}{\partial r} = \frac{12 C_1}{r} \qquad \text{(D-6)}$$

$$\frac{\partial t}{\partial r} = \frac{24 C_1}{d_2} \qquad \text{(D-7)}$$

Combining (D-5) and (D-7):

$$C_1 = \frac{491.472\ Q\ d_2}{24\ \pi\ d_2\ \ell\ k}$$

$$C_1 = \frac{20.478\ Q}{\pi\ k\ \ell} \qquad \text{(D-8)}$$

Combining (D-2), (D-3), and (D-8):

$$\frac{-k\ C_1}{r_1} + h_1\ [C_1\ \ell n r_1 + C_2] = h_1\ t_{NH_3} \tag{D-9}$$

$$C_2 = t_{NH} - C_1\ \ell n\ \frac{d_1}{24} + \frac{24kC_1}{h_1 d_1} \tag{D-10}$$

Particular solution:

$$t = \frac{20.478\ Q}{\pi\ k\ \ell}\ \ell n\left(\frac{r}{12}\right) + t_{NH_3} - \frac{20.478\ Q}{\pi\ k\ \ell}\ \ell n\left(\frac{r_1}{12}\right) + \frac{24k}{h_1 d_1}\ \frac{20.478\ Q}{\pi\ k\ \ell} \tag{D-11}$$

$$t = t_{NH_3} + \frac{20.478\ Q}{\pi\ k\ \ell}\left[\ell n\left(\frac{d}{d_1}\right) + \frac{24K}{h_1 d_1}\right] \tag{D-12}$$

or, conversely,

$$h_1 = \frac{24k}{d_1\left[\frac{\pi\ k\ \ell}{20.478\ Q}\left(t - t_{NH_3}\right) - \ell n\left(\frac{d}{d_1}\right)\right]}\ \text{Btu/hr-ft}^2\text{-°F} \tag{D-13}$$

This analysis has been programmed (for use with a Texas Instruments SR-52 calculator) with these equations including the constants required to convert input tube dimension in inches to dimensions in ft. To appreciate the form of the equations without the constants, Eqs. (D-12) and (D-13), if written for radii to be input in feet, are as follows:

$$t_2 = t_{NH_3} + \frac{Q}{A_1}\left(\frac{r_1}{k}\ \ell n\ \frac{r_2}{r_1} + \frac{1}{h_1}\right) \tag{D-11a}$$

or, conversely,

$$\frac{1}{h_1} = \frac{t_2 - t_{NH_3}}{Q/A_1} - \frac{r_1}{k}\ \ell n\ \frac{r_2}{r_1}\ \text{Btu/hr-ft}^2\text{-°F} \tag{D-12a}$$